Image Cover Sheet

CLASSIFICATION	SYSTEM NUMBER
UNCLASSIFIED	155549

TITLE

ESTIMATION OF TARGET ANGULAR POSITION UNDER MAINBEAM JAMMING CONDITIONS

System Number:

Patron Number:

Requester:

Notes:

DSIS Use only:

Deliver to: FF

National Defence / Défense nationale

ESTIMATION OF TARGET ANGULAR POSITION UNDER MAINBEAM JAMMING CONDITIONS (U)

by

Mylène Toulgoat and Ross M. Turner

DEFENCE RESEARCH ESTABLISHMENT OTTAWA
REPORT NO. 1281

Canada

December 1995
Ottawa

National Defence
Défense nationale

ESTIMATION OF TARGET ANGULAR POSITION UNDER MAINBEAM JAMMING CONDITIONS (U)

by

Mylène Toulgoat and Ross M. Turner
Maritime Radar Group
Surface Radar Section

DEFENCE RESEARCH ESTABLISHMENT OTTAWA
REPORT NO. 1281

PCN
01A01

December 1995
Ottawa

Abstract

A phased-array multifunction radar (MFR) with an agile pencil beam will invariably employ a monopulse system for precise angle measurement. Such a monopulse system has three receiver channels, one channel for each of the sum, azimuth and elevation difference beamformers. This report considers a modest expansion of the number of receiving channels from three to five channels. The five channels comprise the sum channel beamformer and each half of the two difference beamformers. These five channels form an adaptive array which can be used to provide mainbeam nulling of jammers. A new algorithmic approach to mainbeam jammer nulling and target angle estimation is applied to this five-element adaptive array. With this algorithm, the jammer subspace is first evaluated by sampling at ranges where the target is absent (e.g. beyond the maximum range of targets or during a quiet period when the radar is not transmitting). Data vectors are then processed to remove the jammer thus allowing the target to be detected. Finally a high resolution technique, Multiple Signal Classification (MUSIC), is used to estimate the target Direction-Of-Arrival (DOA) from the processed data vectors. The model used in the MUSIC technique takes into account the fact that the jammer has been cancelled in the target data vector. The performance of this algorithm is evaluated through simulations and compared with the Corrected Adaptive Monopulse (CAM) [3,4] for a typical X-band phased array. The new algorithm provides more accurate estimates than CAM when the target is close to the jammer, at the expense of a large computational load.

Résumé

Un radar multifonction dont l'antenne est de type réseau à balayage électronique utilise un système de monopulse pour obtenir avec précision la position angulaire de la cible. Un tel système de monopulse se compose de trois canaux de réception, soit le canal du faisceau somme, la canal du faisceau différence en azimut et celui du faisceau différence en angle de site. Ce rapport étudie une configuration de l'antenne comprenant cinq sous-réseaux dont le canal somme et chaque moitié des faisceaux différences. Ces cinq sous-réseaux forme une antenne adaptative qui peut être utilisée pour l'annulation de brouilleurs dans le lobe principal de l'antenne radar. Nous proposons une nouvelle approche pour annuler le brouilleur dans le lobe principal de l'antenne et pour estimer la position angulaire de la cible en utilisant cette antenne adaptative. En premier lieu, le sous-espace de brouillage est évalué en échantillonnant à des cellules de portée où la cible est absente. Ensuite, le brouilleur est éliminé des données comprenant la cible permettant ainsi la détection de celle-ci. Finalement une technique de haute résolution, appelée MUltiple SIgnal Classification (MUSIC), est appliquée aux vecteurs de données débarrassés de la composante de brouillage, de façon à estimer la position angulaire de la cible en utilisant les vecteurs de données débarrassés du brouillage. Le modèle utilisé dans la technique MUSIC tient compte du fait que le brouilleur a été annulé dans les vecteurs de données contenant la cible. La performance de cet algorithme est évaluée à l'aide de simulations et comparée avec celle de la technique monopulse adaptatif corrigé (CAM) [3,4] pour une antenne réseau typique émettant à la bande X. Le nouvel algorithme donne des estimés plus précis que la technique CAM lorsque la cible est près du brouilleur, au coût d'une plus grande complexité de calcul.

Executive Summary

A multifunction phased array radar (MFR) system would significantly increase the self-defence capability of Canadian war ships. Such a system is currently under consideration for the midlife retro-fit of the Canadian Patrol Frigate (CPF).

The work reported here aims at improving the ECCM capability of the MFR to deal with the problem of mainbeam jamming. This will improve the probability of successfully engaging an attacking missile and therefore the overall probability of ship survival.

Jamming of radar systems via the antenna mainbeam can seriously degrade both the detection of the target and the monopulse angle estimation. Thus jamming can provide a crucial advantage to enemy forces if radar Electronic-Counter-Counter-Measures (ECCM) are not effective. Adaptive nulling provides an effective ECCM but at the cost of increased equipment complexity and capability. There are two major cost factors: (1) the requirement for high quality multiple receiver channels and (2) the need for a very high speed, real-time, computational capability.

This report presents simulated results on radar performance obtainable with a very small number of receiving channels: five channels in total. An MFR ordinarily has three receiving channels corresponding to the sum, azimuth difference and elevation difference beam forming networks which are required to accurately measure target angle in two angular dimensions. We obtain five channels from the sum and from each half of the azimuth and elevation difference beamformers. Because the provision of additional receiver channels is a major cost increase for an MFR, the number of additional channels has been made as small as possible commensurate with the performance sought.

This report describes two techniques for estimating the target Direction-of-Arrival (DOA) in a mainbeam jamming environment. The first is the Corrected Adaptive Monopulse technique described by Nickel [3,4]; this technique calculates correction values for the standard monopulse

formula when mainbeam jamming is present. The second technique uses a two-step procedure; the jammer component is first evaluated and then removed from the target data vector; the target DOA is then estimated by using a high resolution technique such as MUltiple SIgnal Classification (MUSIC). A non standard version of MUSIC is used that accounts for the modification of the array antenna pattern caused by the nulling in the first step. These two techniques are evaluated by means of computer simulations. It is shown that the modified MUSIC technique provides more accurate estimates than the Corrected Adaptive Monopulse at the expense of a larger computational load.

Contents

List of Figures

1.0 Introduction

The main beam jamming problem arises because of the potential for stand-off, escort or self protection jammers to line up with an attacking missile or aircraft; then both the desired target and the jammer fall within the main beam of the antenna. As engagement of an attacking aircraft or missile requires accurate tracking and target position determination, we are faced with a double problem: (1) detection of the target when it deviates slightly from the jammer position and (2) accurate determination of the target angular position.

An adaptive array can, in principle, be constructed of subarrays made up from the MFR antenna. Such an array is capable of nulling a main beam jammer. However, the nulling action can perturb the slope of the monopulse difference pattern so that inaccurate estimates of target position are obtained. In contrast, when sidelobe nulling is applied to jammers in the sidelobes, the conventional monopulse system works well and the monopulse difference pattern suffers only a negligible distortion.

Several techniques have been proposed to deal with the problem of angle estimation when mainlobe jamming is present. Theil [1] describes a two-step procedure in which adaptive nulling is used to eliminate the jammer for detection only. Once the target is detected and its range determined, a high resolution array signal processing technique such as MUltiple SIgnal Classification (MUSIC) [2] is applied to the target range cell and used to resolve the signal from the jammer. The problem with this technique occurs when the jammer return is very much stronger than the target return; it is then difficult to distinguish a very small signal peak from a close-by and very large jammer peak in the MUSIC angular spectrum. Nickel [3,4] developed a technique called Corrected Adaptive Monopulse (CAM). CAM is based on maximum likelihood processing; the likelihood function is approximated as a quadratic surface which allows an analytical expression for calculating the position of the target with respect to the beam centre. CAM is a very fast technique and works well in many instances; it is, however, subject to large bias errors when the quadratic approximation fails as will be described in this report. The CAM technique includes the effect of jammer nulling in its signal model. Because of its importance

and good performance under many but not necessarily all conditions, a detailed treatment and evaluation of CAM is presented.

This report presents a new approach to the mainbeam jamming problem. A two-step procedure is proposed: jammer nulling followed by target angle estimation. Standard techniques are used for the nulling of the jammer. The novelty of the new approach resides in the technique for estimating the target angular position after jammer nulling and target detection. The basis of this new approach is the inclusion of the effects of jammer nulling on the array manifold and the use of a modified array manifold in the MUSIC algorithm which we call Modified MUSIC or MMUSIC. The modified array manifold has also been used to construct a signal model for maximum likelihood estimation; the results of this study will be reported in a subsequent report. For low elevation targets over the water, the effects of specular multipath can be included in the modified array manifold as described by Bossé, Turner and Lecours [5]. This subject will also be reserved for the aforementioned subsequent report.

A notable aspect of this work is the restriction to a small number of subarrays: five in number. Receiver channels for each subarrays, although expensive, are required for mainbeam nulling. Five subarrays represent a modest expansion over the standard three receiver channels required for monopulse angle estimation.

2.0 Array Configuration

The simulated phased-array antenna is shown in Figure 1. There are approximately 3200 elements arranged in a number of columns. It is assumed that beamforming occurs along columns with two column beamformers: one for the sum pattern (linear Taylor tapering) and the other for the elevation difference pattern (linear Bayliss tapering). There are three beamforming networks for combining the column outputs: the array sum pattern which combines the outputs of the Taylor weighted columns with a linear Taylor weighting; the array azimuth difference pattern which combines the Taylor weighted column ouputs with a linear Bayliss tapering; and the array

elevation difference pattern which combines the Bayliss weighted column difference outputs with a linearly tapered Taylor weighting. The Bayliss coefficients [6] $g_B(i)$, i=1, ..., 64 and the Taylor coefficients [7] $g_T(i)$ i=1, ..., 64 are shown in Figure 2.

The report postulates additional receiver channels which require access to intermediate points in the beamforming networks and modification of beamforming networks for combining column outputs so as to give beamforming outputs, z_1 to z_5 where z_1 and z_3 are the outputs of the left and right side of the array, z_2 is the sum pattern output, z_4 and z_5 are the outputs of the upper and lower halves of the array. This adaptive array antenna is shown in Figure 3.

3.0 Signal and noise characteristics

Radar systems usually transmit pulsed signals that are narrowband with respect to the carrier frequency. Since the targets of interest are in the far field, the received signals are plane waves. The data vector, $\mathbf{z}_k$, describes the signals as received by the antenna array, where the k^{th} component of $\mathbf{z}_k$ is the complex signal out of the k^{th} receiving element. In the case where subarrays are formed as described in section 2.0, the components of $\mathbf{z}_k$ are the outputs of the subarrays. We define $\mathbf{z}_k$ for a general array of K elements as:

$$\mathbf{z}_k = \mathbf{s}_k + \mathbf{n}_k$$

with

$$\mathbf{s}_k = b_k \mathbf{a}(\boldsymbol{\omega}_t)$$
$$\mathbf{n}_k = A(\boldsymbol{\omega})\mathbf{j}_k + \mathbf{nr}_k$$

where b_k is the target complex amplitude, $\omega_t=(u_t,v_t)$ is the target direction in azimuth and elevation, $\mathbf{j}_k=[j_1(t_k), ..., j_L(t_k)]$ is the jammer vector with $j_i(t_k)$ being the complex gaussian amplitude of the i^{th} jammer at time t_k, and L is the number of jammers. The quantity, $\mathbf{nr}_k$, is the receiver noise vector with mutually independent components. Its power is $E\{\mathbf{nr}_k^2\}=K\sigma^2$ where K is the number of array elements. The sampling rate is selected such that the quantities $j_i(t_n)$ and

$j_i(t_{n+1})$ are statistically independent. The matrix $A(\omega)$ represents the directions of the jammers with $A(\omega)=[\mathbf{a}(\omega_1), ..., \mathbf{a}(\omega_L)]$. The quantity $\mathbf{a}(\omega_i)$ is a deterministic vector representing the direction of arrival of the i^{th} signal. The vector $\mathbf{a}(\omega_i)$ is given by:

$$\boldsymbol{a}(\boldsymbol{\omega}_i) = [\alpha_1 \exp(j\ \psi_1(\boldsymbol{\omega}_i)), \ldots, \alpha_K \exp(j\ \psi_K(\boldsymbol{\omega}_i))]$$

where α_k, k=1, ..., K, are gain coefficients depending upon the weighting applied to the k^{th} element, $\psi_k(\omega_i)$ is the phase shift caused by the i^{th} signal, located at ω_i, on the k^{th} element.

The phase adjustment reduces to the usual formula for a planar array,

$$\psi_k(\omega_i)=\xi(x_k u_i+y_k v_i).$$

where

$$u_i=(\cos\phi_i)\sin\theta_i,$$

$$v_i=\sin\phi_i,$$

with θ_i and ϕ_i being, respectively, the azimuth angle and the elevation angle of the i^{th} signal, and ξ being equal to $2\pi/\lambda$.

4.0 Methodology for Performance evaluation

Three scenarios are used in the performance evaluation of the two techniques presented here. The first scenario evaluates the algorithms when a mainbeam jammer is present while the other two scenarios evaluate the techniques for sidelobe jammers with different Jammer-to-Noise Ratios (JNR). In each of these scenarios, the array is steered at $\omega=(0°,0°)$. The signal is in the mainlobe, not necessarily at the steering position, with a Signal-to-Noise (SNR) of 0 dB at the element level. In the following three scenarios, JNR levels are specified at the array element output.

Mainbeam jamming scenario:

The jammer is located in the mainbeam at $\omega=(-.3°,-.6°)$ with a Jammer-to-Noise Ratio (JNR) of 25 dB.

Medium level sidelobe jamming scenario:

The jammer is located in the sidelobes at ω=(6°,10°) with a JNR=25 dB.

High level sidelobe jamming scenario:

The jammer is located in the sidelobes at ω=(6°,10°) with a JNR=70 dB.

5.0 Nulling techniques: SMI compared with Eigendecomposition

Two techniques are considered for nulling jamming: Sampled Matrix Inversion (SMI) and eigendecomposition. SMI is a classic technique [8] that results in maximizing the signal-to-noise-plus-jamming-ratio (SNJR). In eigendecomposition, the interference-only sample covariance matrix is decomposed into its eigenvectors. The largest eigenvalue and its associated eigenvector are identified with the jammer and used to form a projection matrix, P, for projecting the antenna steering weight vector, w_s, into a space orthogonal to the jammer space.

Figures 4a and 4b show the antenna patterns for the mainbeam jamming scenario along the axes, θ_{el} = -0.6 and θ_{az} = -0.3, respectively. Two different adapted antenna patterns are shown: the first obtained by using the SMI method, the second by using eigendecomposition. Both patterns are very similar in the main beam region with a null in the jammer direction and reduced gain in the target direction. Eigendecomposition produces a little more gain on one side of the null in the main beam and considerably lower sidelobes , also on the same side of the null for the two cuts shown. It is evident from these results that the five subarray configuration is able to create a null in the direction of a mainbeam jammer but then the mainbeam is adversely affected, creating errors when using monopulse. In both sidelobe jamming scenarios, the nulling does not adversely affect the sidelobes.

6.0 Direction of Arrival Estimation

In this report, two different approaches are used to determine the target angle-of-arrival with the adaptive array. The first approach uses the CAM formula of Nickel. This formula gives the correction values for the slope and zero-crossing of the adapted monopulse response. The second approach applies high resolution techniques to the adaptive array antenna to estimate the target direction. In the latter case, the estimation is done in three steps: first, the jammer subspace is estimated from a training set; second, the jamming component is removed from the data vector that contains the target plus jammer plus noise; third, a high resolution technique is used to estimate the target DOA from processed data vectors.

Both approaches require the estimation of the jammer subspace. The jammer subspace is estimated from the jammer covariance matrix; the latter is estimated using samples of the signal taken at range cells where the target is not present. The covariance matrix, Φ_J, is calculated by:

$$\Phi_J = \frac{1}{S}\sum_{i=1}^{S} \mathbf{z}_i \mathbf{z}_i^H$$

where S is the number of samples and $\mathbf{z}_i$ is the i^{th} data vector (taken at the subarray outputs) that contains jammer plus noise only. The jammer subspace can be obtained from the covariance matrix by several different techniques: for example, the Sample Matrix Inversion (SMI) or a projection technique. The latter requires the determination of the jammer subspace by processing the columns of the covariance matrix. This processing can be either eigendecomposition, Gram-Schmidt orthogonalization or another technique that gives an orthogonal basis. A projection matrix, P, is then calculated from this basis, V, by:

$$P = I - VV^H$$

In the CAM formula, this projection matrix is used to calculate the adapted monopulse characteristic as well as the correction values for the slope and zero crossing. When high resolution techniques are used to estimate the target DOA, the projection matrix, which is orthogonal to the jammer subspace, is used to process the data vectors. The jamming component is removed from the data vector by projecting the data vector containing the target plus jammer plus noise into a subspace orthogonal to the jammer subspace

$$\mathbf{z}' = P\mathbf{z}$$

Here $\mathbf{z}'$ is a new, processed, data vector in which the jammer is nulled (or at least attenuated). When the Sample Matrix Inversion technique is used to cancel the jammers, the jammers are removed from the data vectors by multiplying them by the inverse of the covariance matrix to obtain a modified data vector, $\mathbf{z}'$. A high resolution technique such as Maximum-Likelihood or MUSIC is used to estimate the DOA of the target from the modified data vector. Since these techniques are based on the correlation between a model of the target and the data vector, the model of the target is modified by the same projection matrix (or inverse of the covariance matrix) as was used for processing the data vector.

This report studies the CAM formula and the MUSIC estimator. Two different techniques have been considered for the estimation of the jammer subspace: Sample Matrix Inversion and eigendecomposition. The next section describes the CAM technique.

7.0 Conventional and Corrected Adaptive Monopulse

The MFR system uses amplitude monopulse to determine target location. Amplitude monopulse uses the sum and difference antenna patterns. The sum pattern has a peak in the direction of the steered beam while the difference pattern has a null. When a target is detected, its angular position is only known to the width of the sum pattern. A precise estimate of the target position with respect to the center of the sum beam is found by forming the ratio of the difference to the sum pattern. One obtains a quasi-linear curve which can be calibrated to give

an accurate estimate of the deviation of the target from the sum pattern peak. The conventional monopulse formula is given by:

$$\hat{u} = u - \sigma_u \, Re[\mathbf{d}_u^H \mathbf{x} / \mathbf{a}(\boldsymbol{\omega})^H \mathbf{x}] = u - \sigma_u \, Re[\Delta_{az} / \Sigma]$$

$$\hat{v} = v - \sigma_v \, Re[\mathbf{d}_v^H \mathbf{x} / \mathbf{a}(\boldsymbol{\omega})^H \mathbf{x}] = v - \sigma_v \, Re[\Delta_v / \Sigma]$$

where $\hat{\boldsymbol{\omega}} = (\hat{u}, \hat{v})$ is the estimate of the target direction, $\boldsymbol{\omega} = (u, v)$ is the steering direction, $\mathbf{d}_u$, $\mathbf{d}_v$ are the weight vectors for difference beamforming with respect to the u- and v- axis and σ_u, σ_v are fixed slope correction values. The sum and difference channel responses for the simulated MFR system, given in Figure 5 a, b, c, are used to calculate the monopulse error for the target DOA.

When mainbeam nulling is used, the estimation of the target position with conventional monopulse is impossible. One can use the adapted difference and sum patterns for this purpose; however, it has been shown that the zero position and the slope of the difference pattern as well as the shape of the sum pattern are severely distorted whenever mainbeam jammers are present.

Lin and Kretschmer [9] have proposed a method for using adapted monopulse calibration curves with mainbeam jamming. The calibration curve, in effect, compensates for distorsions in the sum and difference patterns caused by nulling of the main beam jamming. Their treatment was restricted to two dimensional geometry, with the array, jammers, and steering direction all lying in the same plane. This technique does not appear to be useable with three dimensional geometry where it is necessary to estimate both elevation and azimuth angle. Because of the coupling between azimuth and elevation in the calibration curves, it does not seem possible to obtain unique calibration curves for azimuth and elevation when these are not known a priori. However, an iterative approach is possible in which we assume elevation at the centre of the beam for the azimuth calibration curve, and vice versa for the elevation calibration curve. These two estimates are then used to produce two new calibration curves more accurate than the previous one and so on. This procedure has not been treated; however, this approach will be examine in a future study.

The next two sections present two different techniques for direction finding when mainbeam jamming is present. The first one, the CAM formula [3,4], gives the correction for the slope and zero crossing of the adapted monopulse ratio in presence of jamming. This technique is simple to implement and requires a number of computations comparable with those of the conventional monopulse technique. However, CAM sometimes experience large bias errors when the jammer and signal are too closely spaced. The second technique is a new spectral estimator based on the MUSIC technique. This technique is very precise but, as it requires a search for a maximum in a two-dimensional space, it is computationally very intensive.

7.1 Derivation of the CAM technique

The CAM formula calculates the correction values for the slope and zero crossing of the adapted monopulse ratio. It requires determining the vector ω that maximizes the following likelihood function:

$$P(\boldsymbol{z}\,|\boldsymbol{S}+\boldsymbol{N}) = \frac{(\boldsymbol{z}-b\boldsymbol{a}(\omega))^H R^{-1}(\boldsymbol{z}-b\boldsymbol{a}(\omega))}{\pi^{-K}|R^{-1}|}$$

The estimate of ω is a function of the data vector **z** and the covariance matrix of the jamming signal. Nickel [3,4] showed that maximizing the likelihood function is equivalent to maximizing the scan pattern:

$$S_{scan}(\omega) = |\boldsymbol{w}_a(\omega)^H \boldsymbol{z}|^2$$

with

$$\boldsymbol{w}_a(\omega) = \frac{P\,\boldsymbol{a}(\omega)}{(\boldsymbol{a}(\omega)^H P \boldsymbol{a}(\omega))^{\frac{1}{2}}} \quad .$$

P is the projection matrix orthogonal to the jammer subspace. The corrected monopulse formula is derived from the last equation by a second order Taylor expansion of the logarithm of the scan pattern at the position of its maximum ω_{max}:

$$\begin{bmatrix} \hat{u} \\ \hat{v} \end{bmatrix} = \begin{bmatrix} u \\ v \end{bmatrix} - \begin{bmatrix} F_{uu} & F_{uv} \\ F_{uv} & F_{vv} \end{bmatrix}_{\omega_{max}}^{-1} \begin{bmatrix} F_u \\ F_v \end{bmatrix}_{\omega}$$

$$\begin{aligned} F_u &= Re\left[(\mathbf{d}_{ad,u}^H \mathbf{z}) / (\mathbf{w}_a^H \mathbf{z}) \right] - \mu_u \\ F_v &= Re\left[(\mathbf{d}_{ad,v}^H \mathbf{z}) / (\mathbf{w}_a^H \mathbf{z}) \right] - \mu_v \\ F_{uu} &= \mu_u^2 - \mathbf{d}_{ad,u}^H \mathbf{d}_{ad,u} \\ F_{vv} &= \mu_v^2 - \mathbf{d}_{ad,v}^H \mathbf{d}_{ad,v} \\ F_{uv} &= \mu_u \mu_v - Re[\mathbf{d}_{ad,u}^H \mathbf{d}_{ad,v}] \end{aligned}$$

$$\mathbf{d}_{ad,u} = \frac{P\,\mathbf{d}_u}{(\mathbf{a}^H P \mathbf{a})^{\frac{1}{2}}}$$

$$\mathbf{d}_{ad,v} = \frac{P\,\mathbf{d}_v}{(\mathbf{a}^H P \mathbf{a})^{\frac{1}{2}}}$$

$$\mu_u = Re\{\frac{\mathbf{d}_u^H P \mathbf{a}}{\mathbf{a}^H P \mathbf{a}}\}$$

$$\mu_v = Re\{\frac{\mathbf{d}_u^H P \mathbf{a}}{\mathbf{a}^H P \mathbf{a}}\} \quad ,$$

with $\mathbf{d}_u$ and $\mathbf{d}_v$ being the derivatives of the steering vector relative to u and v respectively. With no jammer present, $\mathbf{d}=\mathbf{d}_{ad}$, P=I, $\mathbf{w}=\mathbf{a}(\omega)$ and the CAM formula reduces to the conventional monopulse formula for the adaptive array antenna. This formula is valid for one frequency. It was shown that when conventional monopulse is used in presence of multipath, better results could be obtained using frequency agility. This problem, of great importance in the context of low angle tracking over water, will be addressed for the CAM formula in a subsequent report.

7.2 Simulation results

In this section, we evaluate the performance of both the Corrected Adaptive and Conventional Monopulse techniques for our MFR configuration. Results are presented for the three scenarios described in the previous section: mainbeam jamming, medium-level sidelobe jamming and high-level sidelobe jamming.

In the simulations, targets can lie anywhere within the mainbeam. Therefore we have to define representative cases to illustrate performance. Thus we move the target across the beam following a preset path that passes through the centre of the array, examining the error in angle estimation for each target position. Two test cases are defined: Test case 1, where the target varies in azimuth (φ=0°), and Test case 2, where the target varies in elevation (θ=0°). Note that in neither of these test cases does the target pass directly through the jammer position.

Test case 1: The target azimuth angle, θ, varies from -0.8° to 0.8° while the elevation angle, φ, is held fixed at 0° (the target position varies along the azimuth axis).

Test case 2: The target elevation angle, φ, varies from -0.8° to 0.8° while the azimuth angle, θ, is held fixed at 0° (the target position varies along the elevation axis).

Results for Mainbeam Jamming

In this scenario, the jammer is at the position (-.3°,-.6°) with a JNR of 25 dB as measured at the element level prior to beamforming. The target is moved across the beam in the azimuth direction (Test case 1) and in the elevation direction (Test case 2). For each target position, the azimuth and elevation angle of the target is estimated by Monte-Carlo simulation with 100 trials for every target position. The signal-to-noise ratio (SNR) is 0 dB as defined at the element level. Therefore, at the output of the sum pattern, the SNR will be 0 dB + 35 dB =35 dB.

Effect of adaptive nulling on the antenna patterns

We start by comparing the unadapted beam pattern with two adapted patterns. The two adapted patterns are obtained by using two different methods to null the jammer: eigendecomposition in the first instance and inversion of the covariance matrix in the second. The adapted antenna patterns are shown in Figure 6, where we see an azimuth cut (Fig. 6a) and an elevation cut (Fig. 6b). In the case of the azimuth cut (Test case 1) the signal passes by the jammer at a reasonably large distance (.6 degree) so that the null at -1.64 degrees is quite far removed from the actual azimuth of the jammer at -.3 degree. In elevation (test case 2) this cut passes much closer to the jammer (.3 degree) so that the position of the elevation null (-.7 degree) is much closer to the jammer elevation position (-.6 degree). Since neither of these antenna pattern cuts passes through the actual jammer position, the deviation of the null position from the jammer position is expected.

The CAM technique is implemented by means of a Taylor expansion at the beam centre where the pattern is assumed to be quadratic. The null positions correspond to regions where the antenna pattern is violently perturbed from that of the assumed smooth quadratic shape; larger errors in angle-of-arrival estimation are expected in these regions.

Angle estimation

When conventional monopulse is used, the jammer position is always given as the target position, ie the jammer succeeded in completely deceiving the system. Therefore, no detailed results in terms of mean and rms errors are presented for this case since the error in target estimation is solely a function of how close the target happens to be with respect to the jammer.

The results for the CAM method are presented in Figure 7 and 8. Here we have plotted both the mean error (ME) and the root-mean-square error (RMSE). As angle estimation follows adaptive nulling, the particular type of adaptive nulling could have an effect on the errors. Therefore, we have plotted the results of eigendecomposition in Fig 7 and Sampled Matrix Inversion in Fig 8. An examination of the results of Figures 7 and 8 lead to the following

observations:

(i) The errors are least for the target near the centre of the beam since the second order approximation to the scan pattern is best at beam center [3,4]. These errors are between .1 and .2 degrees rms corresponding to 5% to 10 % of the two degree beamwidth.

(ii) The mean and rms errors increase as the target approaches the edge of the beam.

(iii) Errors are larger for negative target elevation and azimuth because the target is closer to the jammer which lies in the third quadrant.

(iv) A comparison of the results of Fig 7 with those of Fig. 8 indicates that somewhat better performance is achieved with Sampled Matrix Inversion (SMI) as compared with eigendecomposition.

Sidelobe Jamming Results

Two levels of jamming are considered here; a medium level jamming scenario with JNR =25 dB and a very high level jamming scenario with JNR=70 dB, the JNR values being measured at the array element level. The latter scenario could well drive the front-end of the receiver into saturation. In this analysis, saturation effects are not considered: instead, linear operation is assumed in all cases. Assuming an antenna array sidelobe gain of -10 dBi, the received jammer power in the antenna sum pattern after beamforming would have a JNR of 15 dB in the case of medium level jammer and 60 dB in the case of the high-power sidelobe jammer.

Medium level Sidelobe jamming (JNR=25 dB)

Effect of Nulling on the Adapted Antenna Patterns

In this case, performance should not be much affected by the jammer because of the attenuation of the jammer by the low sidelobes. The use of Conventional Monopulse without jammer suppression gives good results: the mean error is less than ± .05 degree and the RMSE is less than .05 degree in all cases, as shown in Figure 9.

If adaptive nulling is applied, different results will be obtained depending on whether SMI or eigendecomposition is used. The adapted patterns are shown in Figures 10a and 10b. We see that eigendecomposition introduces a null in the mainbeam region at (-1,1) which adversely affects the accuracy of angle estimation. In contrast, SMI does not introduce an accurate null in the mainbeam region; the main beam pattern is relatively unperturbed and more acurate angle estimation is obtained.

Angle Estimation

Figures 11 and 12 give the results for CAM using eigendecomposition and Sampled Matrix Inversion (SMI), respectively. Both the Mean Error and the RMSE have been plotted. An examination of Figures 11 and 12 lead to the following observations:

(i) When eigendecomposition is used to null the jammer, the results are similar to those obtained with a mainbeam jammer because the nulling of the sidelobe jammer introduces a null in the mainbeam.

(ii) In contrast, when SMI is used to suppress the jammer, the DOA estimates are much better. The Mean Error is less than 0.2 degree while the RMSE is less than .15 degree in every case.

(iii) The decrease in performance observed when eigendecomposition is used is explained by the poor performance of projection techniques when the JNR is very low.

High Level Sidelobe Jamming

In this scenario, the jammer is at the position (6°,10°) with a JNR=70 dB, as measured at the element level prior to beamforming. The target is moved across the beam in the azimuth direction (Test case 1) and in the elevation direction (Test case 2). For each target position, the azimuth and elevation angle of the target is estimated by Monte-Carlo simulation with 100 trials for every target position. The signal to noise ratio (SNR) is 0 dB as defined at the element level. Therefore, at the output of the sum pattern, the SNR will be 0 dB + 35 dB =35 dB. Assuming an antenna array sidelobe gain of -10 dBi, the received jammer power in the antenna sum pattern after beamforming would have a JNR of 60 dB.

Effect of adaptive nulling on the antenna patterns

Figures 13 a and 13 b give the antenna pattern around boresight, obtained by two different methods: eigendecomposition and SMI. When jammer suppression is implemented, using eigendecomposition, a null appears in the pattern at approximately (-1.25°,1.25°). Although this null is outside the mainlobe, it still distorts the mainlobe around θ=-1° for Test case 1 and around φ=1° for Test case 2. When jammer suppression is obtained through matrix inversion, the mainlobe is not distorted but a loss of approximately 12 dB in gain is observed.

Angle Estimation

As with mainbeam jamming, the Conventional Monopulse formula fails in locating the target angular position. Figures 14 and 15 give results obtained with CAM for eigen decomposition and SMI respectively. An examination of the results of Figures 14 and 15 lead to the following observations:

(i) As in the mainbeam nulling case, the RMSE error is minimum around $\omega=(0°,0°)$ and is less than 0.05° (2.5 %) for both test cases.

(ii) Large errors occur where the mainbeam is distorted the most.

(iii) The antenna pattern around the boresight was less distorted by the matrix inversion method (the matrix inversion still provides a null at the jammer location (6°,10°)). The results, in this case, are better than those for the eigendecomposition technique.

(iv) When the Sampled Matrix Inversion is used to evaluate the jammer subspace, the RMSE of the estimate of the target's DOA is always less than 0.2 degree (10% of a beamwidth), for all target directions, even those close to the jammer direction.

We note that the error for sidelobe jamming is smaller when JNR=70 dB compared to the case with JNR=25 dB. For the weaker jammer, a null appears in the mainlobe along the axis $\theta=0°$, while there is no null in the mainbeam when JNR=70 dB, as it is shifted outside the mainlobe.

Comparison of all scenarios

The choice of an appropriate technique to evaluate the target DOA depends on the jammer scenario. From the results previously shown, it is clear that conventional monopulse fails when a jammer is in the mainlobe or when a high power jammer is in the sidelobe. On the other hand, when medium level jammer is in the sidelobe, or when there are no jammers, conventional monopulse performs quite well. The RMSE is always less than 0.07° (3.5% of the beamwidth) as shown in Figures 16 and 17 for these scenarios.

CAM is potentially useful for all the scenarios investigated. Figures 18 and 19 show the Mean Error and the RMSE of each scenario for test cases 1 and 2 respectively. Sampled Matrix Inversion was used as the jammer nulling technique since it performs better than eigendecomposition. Figures 18 and 19 present results for all scenarios and for the two test

cases. For the two sidelobe jamming scenarios, performance is very good, with the RMSE being less than .2° (10% of beamwidth) for all targets in the beam. For targets near the centre of the beam, errors are about .1 degree. For the mainbeam jamming scenario, some quite large errors are observed for targets near the jammer position. These large errors correspond to bias errors caused by failure to meet the assumption of a quadratic variation of the likelihood function in the region of the target. We will see that these bias errors are much reduced when MMUSIC is used to process the data.

8.0 The Modified MUSIC (MMUSIC) Technique

A new technique, modified MUSIC or MMUSIC, is introduced to deal with some of the deficiencies of the CAM technique, which are poor performance when the jammer and target are close together. In this case, the mainbeam pattern deviates significantly from the parabolic shape assumed in the CAM formula.

The new MMUSIC technique is a three-step process: the jammer subspace is first estimated; the jammer is then nulled by projecting the array data vector into a space orthogonal to the jammer; the target position is then estimated by using MUSIC with a model vector. This model vector has been modified to account for the effect of jammer nulling by multiplying the standard model vector by the same projection matrix as was used to null the jammer.

Estimation of the jammer subspace:

1) Sample the range cells where the target is absent to obtain S data vectors with jamming signal only, $\mathbf{z}_i$, i=1,...,S.

2) Form the covariance matrix of the jamming signal, Φ:

3) Perform an eigendecomposition on the covariance matrix, Φ. Thus, we obtain

$$\Phi = \frac{1}{S}\sum_{i=1}^{S} z_i z_i^H$$

K eigenvalues λ_i i=1,...,K.

K associated eigenvectors e_i i=1,...,K.

We used the eigenvector associated with the strongest eigenvalue since we have one jammer in each scenario. The jammer subspace is calculated from the eigendecomposition by

Jammer subspace = $e_i e_i^H$, where e_i is the eigenvector associated with the largest eigenvalue.

Suppression of jamming signals in the data vector:

We calculate projection matrix, P_1, which represents a subspace orthogonal to the jammer subspace:

$$P_1 = I - e_1 e_1^H$$

Each data vector, **z**, containing the signal plus jammer plus noise is modified by that projection matrix in order to obtain a new data vector, **z'**, orthogonal to the jammer subspace,

$$z' = P_1 z$$

Evaluation of the MUSIC estimator:

This new data vector, **z'**, is then used to form a covariance matrix, R,

$$R = \sum_{i=1}^{N} z' z'^H$$

which in turn is decomposed through eigendecomposition to obtain the signal subspace. A new projection matrix, P_2, is calculated from this subspace and used to calculate the MUSIC estimator as follows:

$$MUSIC(\omega) = \left(\frac{\mathbf{f}(\omega)^H P_2 \mathbf{f}(\omega)^H}{|\mathbf{f}(\omega)|^2}\right)^{-1}$$

where $\mathbf{f}(\omega)$ is a model of the steered target. Since the data vector has been modified by a projection matrix, the model should also be modified by the same projection matrix, P_1. Thus $\mathbf{f}(\omega)=P_1\,\mathbf{a}(\omega)$.

Two characteristics of the technique are very important. First, the data vectors used to form the second covariance matrix are data vectors in which the jammer is nulled. This insures that the MUSIC estimator will be maximum in the signal direction. The second point concerns the model used for the MUSIC estimator. Since the data vectors are modified by a projection matrix (i.e. projected into a subspace orthogonal to the jammer subspace), the model has to be modified in the same manner. The estimator obtained has the form

$$\frac{\mathbf{a}^H P_1 \mathbf{a}}{\mathbf{a}^H P_1 P_2 P_1 \mathbf{a}} \quad ,$$

where P_1 is orthogonal to the jammer subspace and P_2 is orthogonal to the signal subspace modified by P_1. When the quantity $\mathbf{a}$ approaches the signal direction, the quantity $P_2P_1\mathbf{a}$ approaches 0 and, consequently, the estimator becomes very large. When the vector $\mathbf{a}$ approaches the jammer direction, the estimator tends to 0/0. However, an examination of the limiting behavior in the vicinity of the singular point shows that the estimator is well behaved and finite in the region of the singular point. The peak value is small compared to that observed in the signal direction.

8.1 Simulation results for MMUSIC

In this section, we evaluate the performance of Modified MUSIC (MMUSIC) techniques for our simulated array. Results are presented for the three scenarios described in the previous section: mainbeam jamming, medium level sidelobe jamming and high level sidelobe jamming. We use the same test cases as for the General and Conventional Monopulse formulas: Test case 1, where the target varies in azimuth (φ=0 degree), and Test case 2, where the target varies in elevation (θ=0 degree).

Contour plots

Figure 20 gives contour plots of the MMUSIC estimator for the three different scenarios, when the target is at the steering direction, i.e. ω=(0°,0°). Figure 20a gives the contour plot for the mainbeam jamming scenario. We see a maximum at the target location and a null at the jammer location. In Figures 20b, 20c and 20d, there is no null in the mainbeam since the jammer is either outside the mainlobe or absent. As in the previous three cases, there is a peak at the target location.

Angle Estimation

Figure 21 gives the results for the three scenarios, for Test case 1 (azimuth cuts). In this case the mean error is no larger than 0.03 degree while the RMSE is smaller than 0.07 degree. Figure 22 gives similar results for Test case 2 (elevation cuts). In this case, the mean error is also very low (0.035°), while the RMSE is slightly larger than for test case 1, with a peak RMSE of 0.2 degree. The MMUSIC algorithm performs well in the three scenarios investigated, because the target model includes the effects of jammer rejection.

Comparison of MMUSIC, CAM and Conventional Monopulse

Comparing the results of MMUSIC with those obtained with CAM , it is obvious that the MMUSIC algorithm gives much better estimates of the DOA of the target in diverse environments than either CAM or the Conventional Monopulse formula. This advantage is most pronounced around the nulls in the mainlobe. The better performance of the MMUSIC estimator results from the use of a precise model which incorporates the effect of jammer nulling on the array manifold. In contrast, the CAM formula uses a parabolic approximation to the mainbeam pattern even though this is distorted by the jammer nulling. From the computational point of view, the MMUSIC algorithm is fairly computationally intensive, especially in the case of a two-dimensional search. In this case, the estimator has to be evaluated for every position in the mainbeam where the target is expected. For a resolution of Δ_{az} in azimuth and Δ_{el} in elevation, the estimator has to be evaluated $N_{az}N_{el}$ times with $N_{az}=BW_{az}/\Delta_{az}$ and $N_{el}=BW_{el}/\Delta_{el}$. This large computational load may prevent us from using the MMUSIC algorithm for real-time operation. In contrast, the CAM formula offers many advantages for real-time operation. The formula is evaluated at one point instead of $N_{az}N_{el}$ points for the MMUSIC method. It is suggested that MMUSIC be combined with the CAM formula in an hybrid technique to take advantage of both the high resolution provided by MMUSIC and the computational savings provided by CAM. In this hybrid algorithm, the CAM method could be used to provide an approximate estimate of the target angular position before the MMUSIC algorithm is used around this value to determine a better estimate of the target angular position. This procedure should restrict the two-dimensional search of the MMUSIC algorithm to a smaller area and lower the computational load of the algorithm. Another way of reducing the computational load of the MMUSIC algorithm is the use of a look up table technique for the model. Studies of these alternatives approaches are currently underway.

All the results presented so far were obtained for a large SNR at the element level, which may not reflect a practical situation. The next section considers target and jammer levels that are more typical of an MFR configured to detect small targets at as long a range as possible.

9.0 Comparison of MMUSIC and CAM formula for detecting small targets

In this section, we evaluate the performance of MMUSIC and CAM formula for an MFR tracking a small target. Two factors have to be taken into account: the level of SNR required for detection and the level of JNR in the mainlobe of the antenna. The latter factor is important since projection techniques perform better when the JNR is high. We assume a gain in the sum channel of approximately 35 dB while the gain in the difference channel is assumed to be 32 dB. A typical SNR of 18 to 23 dB is required for the detection of a target. Under these circumstances, the SNR at the element level is between -17 dB and -12 dB with an antenna gain of 35 dB. Simulation results are obtained for a target located at (.2°,.4°) and a jammer at (-.3°,-.6°). The array is steered to (0°,0°). Figures 23 and 24 show the Mean Error and RMSE versus JNR for SNR=-17 dB and SNR=-12 dB respectively, for both the CAM formula and the MMUSIC algorithm. From these figures, we see that both the Mean Error and the RMSE are constant if the JNR is sufficiently high. For a SNR=-17 dB, the RMSE in azimuth is approximately .35° for the CAM formula and approximately .15° for the MMUSIC algorithm. The RMSE in elevation is around .65° for CAM and .25° for MMUSIC. When the SNR=-12 dB, the RMSE in azimuth drops to .2° for the CAM formula and to .05° for the MMUSIC algorithm. The RMSE in elevation is about .35° for CAM (large JNR) while it is less than .15° for MMUSIC. There is clearly a large improvement in performance when using the MMUSIC technique for large JNR. When the JNR is low, the performance of MMUSIC deteriorates relative to CAM. This is due to the jammer nulling technique used in MMUSIC. It is well known that projection techniques, such as eigendecomposition, are not performing very well for low JNR. It is expected that, the use SMI instead of eigendecomposition to null the jammer would improve the performance of MMUSIC. The effect of using different nulling techniques in the MMUSIC method will be presented in a future report.

Figure 25 gives the Mean Error and the RMSE versus the SNR when a jammer of JNR=25 dB is present in the mainbeam. As the SNR increases, the estimate of the target DOA improves. In certain tracking modes, the dwell time can be increased, providing more pulses for coherent integration. Moreover, frequency agility could be used to average the different estimates

obtained from different bursts, thus providing a better estimate of the target DOA. Finally, estimates of the DOA of targets with larger cross sections or at closer range will be better because of the higher SNR in the receiver. The implications of these factors will be addressed in a subsequent report.

10.0 Conclusions

In this report, we have presented two techniques that estimate the target DOA in presence of mainbeam jamming. The first technique is the CAM formula developed by Nickel [3,4], the second, a modified version of the MUSIC algorithm. These two techniques require the use of an adaptive array antenna. Since many MFR antennas are not subarrayed, we suggested the use of the outputs of the sum and the azimuth and elevation difference channels to form an adaptive array antenna. This adaptive antenna has four degrees of freedom when nulling jammers in the mainbeam. Three scenarios were evaluated: one with a mainbeam jammer, two with a sidelobe jammer. It was shown that, in all cases, the MUSIC estimator offered more accurate estimates of DOA than the CAM formula, but at the expense of a larger computational load. Future work will evaluate the use of an hybrid configuration to overcome this problem. The CAM formula will be used to obtain a first estimate of the target DOA and then a two-dimensional search around this value will be performed using the MMUSIC algorithm. We are also investigating the steepest ascent algorithm to find the maximum of the estimator. Future work will include the effect of multipath on each of the techniques and the use of frequency agility, as well as the use of more subarrays, to improve the quality of the estimates.

11.0 Acknowledgements

The authors would like to acknowledge the work performed by Ed Riseborough of DREO and Anna Wilkinson of AIT Corporation in the preparation of some of the figures.

12.0 References

[1] Theil, A., "On Combining Adaptive Nullsteering with High Resolution Angle Estimation under Mainlobe Interference Conditions", IEEE International Radar Conference, 1990, pp. 295-297.

[2] Schmidt, R.O. "Multiple Emitter Location and Signal Parameter Estimation", IEEE Trans., Vol. AP-24, 1986, pp.276-280.

[3] U. Nickel, "Monopulse estimation with adaptive arrays", IEE Proceedings-F, Vol.140, No.5, October 1993, pp. 303-308.

[4] U. Nickel, "Angle Estimation with Adaptive Phased Array Radar Under Mainbeam Jamming Conditions", AGARD CP-488 (AGARD AVP Symposium on ECCM for Avionic Sensors and Communication Systems).

[5] Bossé, E, Turner, R.M. and Brookes, D., "Improved radar tracking using a multipath model: maximum likelihood compared with eigenvector analysis", IEE Proc. Radar, Sonar Navig., Vol. 141, No.4, August 1994.

[6] Hansen, R.C., "Microwave Scanning Antennas, Volume 1: Apertures", Academic Press, New York and London, 1964.

[7] Hansen, R.C., "Array Pattern Control and Synthesis", IEEE Proceedings, Volume 80, No.1, January 1992.

[8] Reed, I.S., Mallett, J.D., Brennan, L.E., " Rapid Convergence Rate in Adaptive Arrays", IEEE Trans. Vol. AES-10, No.6, November 1974, pp.853-864.

[9] Feng-Ling C. Lin and Frank F. Kretschmer, Jr., "Angle Measurements in the presence of mainbeam interference", IEEE International Radar Conf., 1990, pp.444-450.

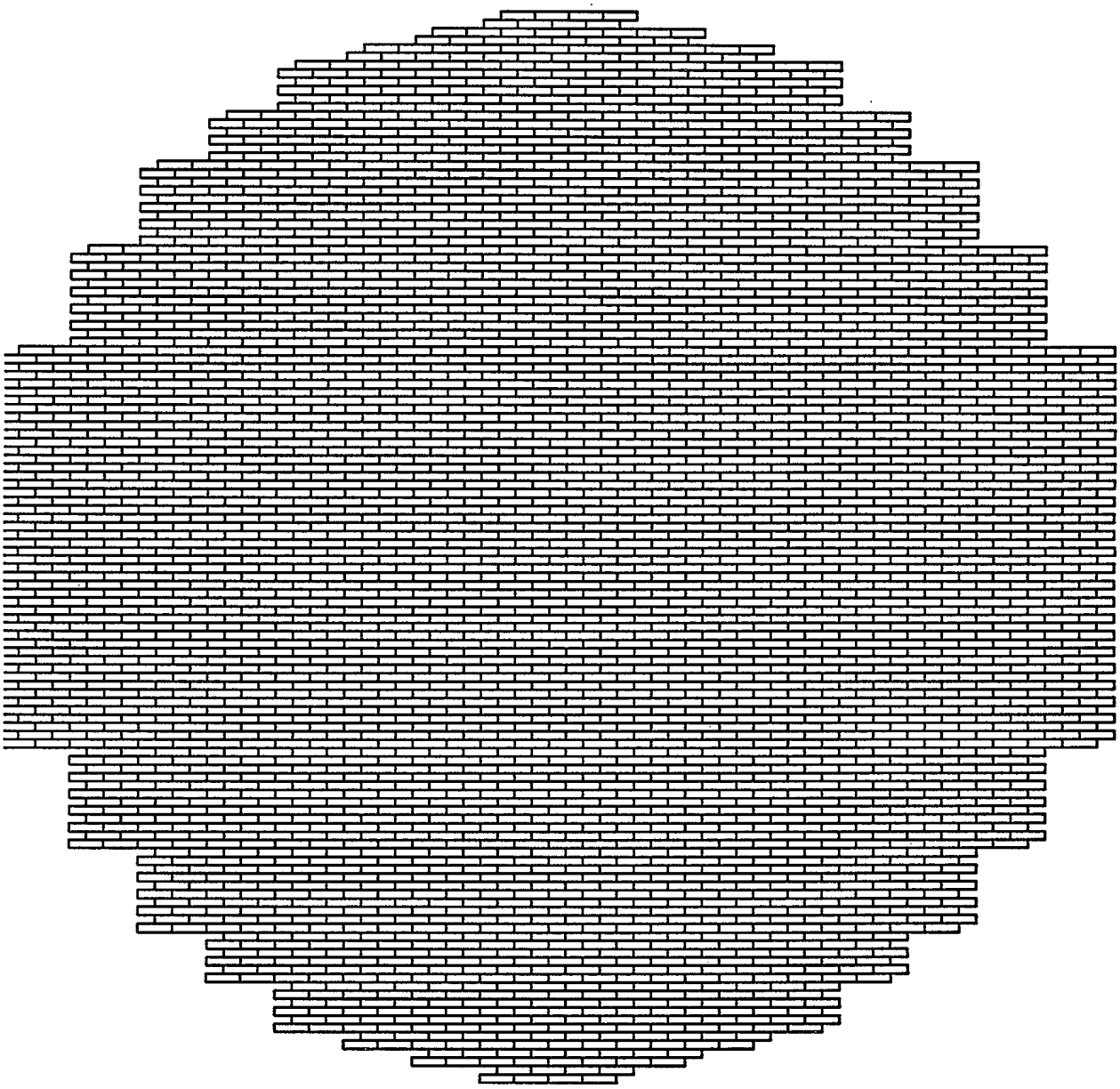

Figure 1 Simulated phased array antenna.

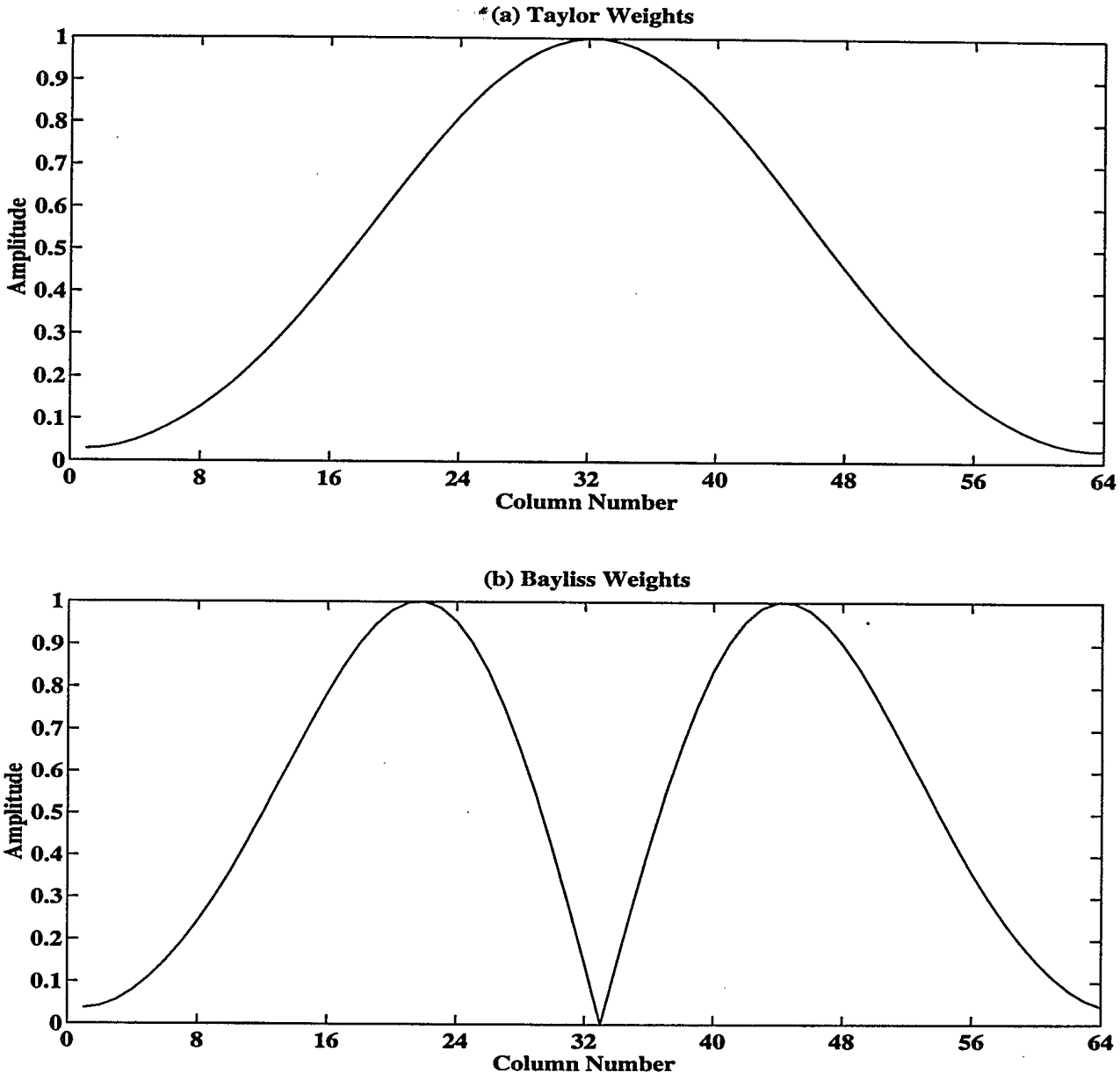

Figure 2 Bayliss and Taylor coefficients.

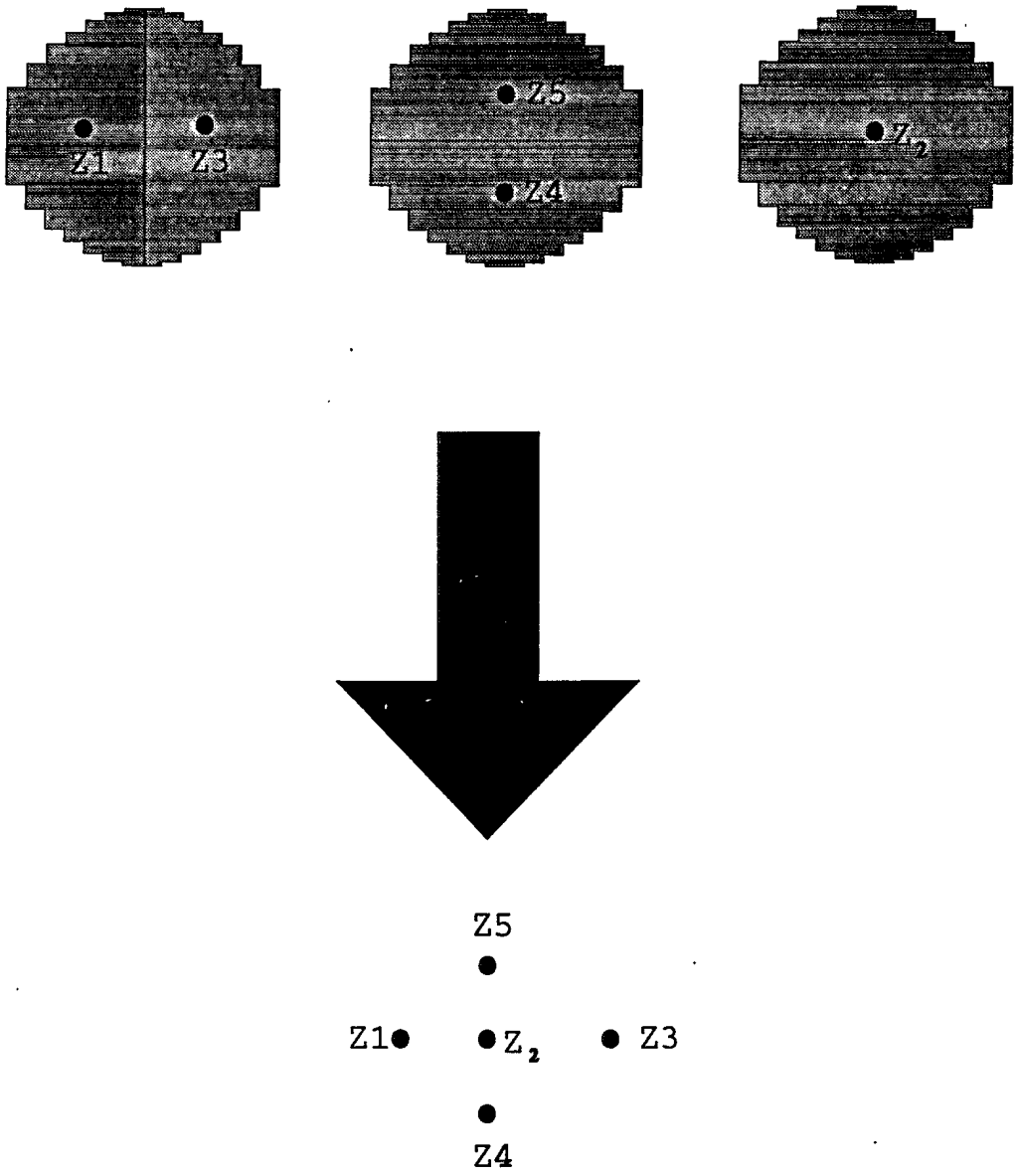

Figure 3 Adaptive array antenna.

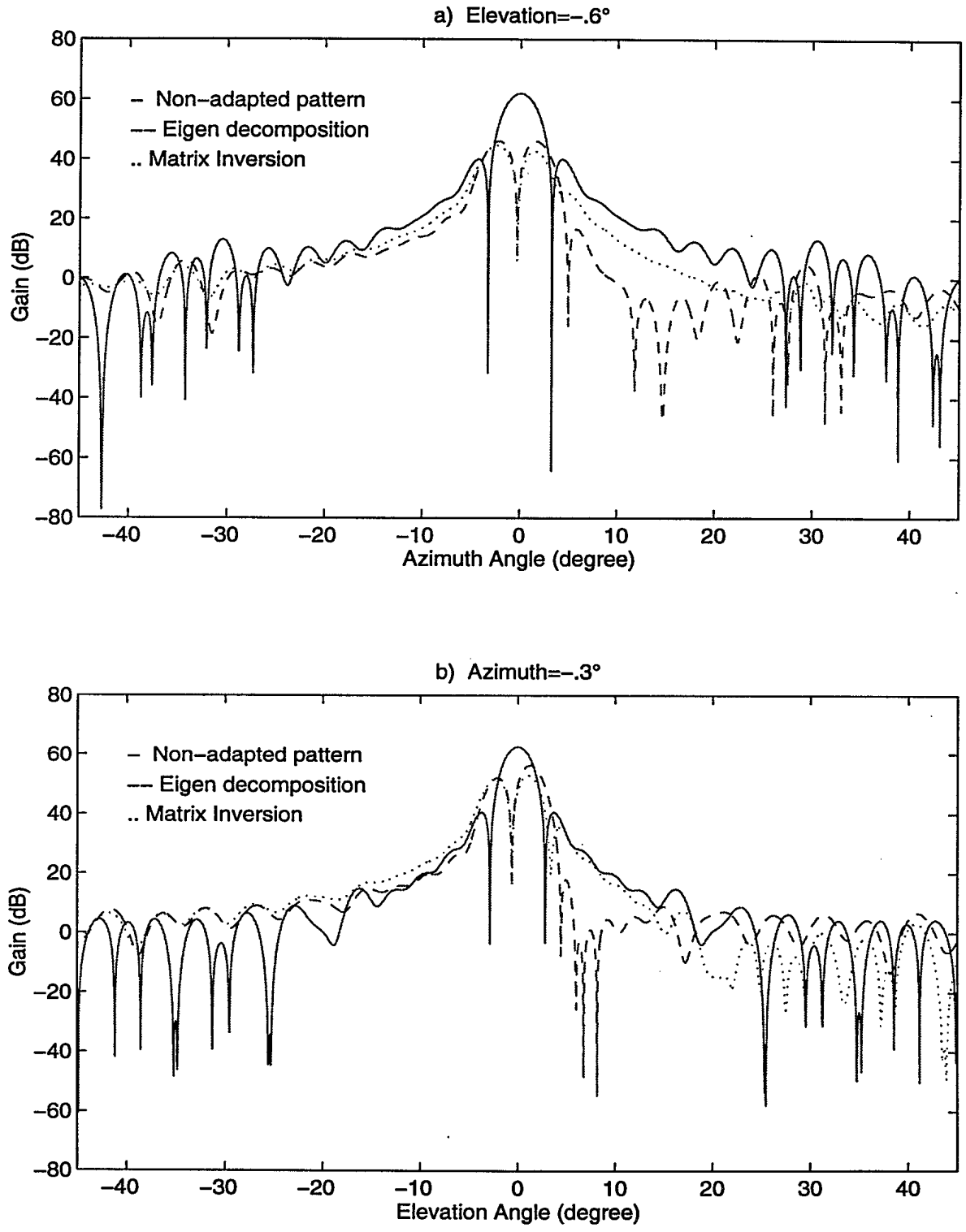

Figure 4 Adapted Antenna patterns for mainbeam jamming scenario.

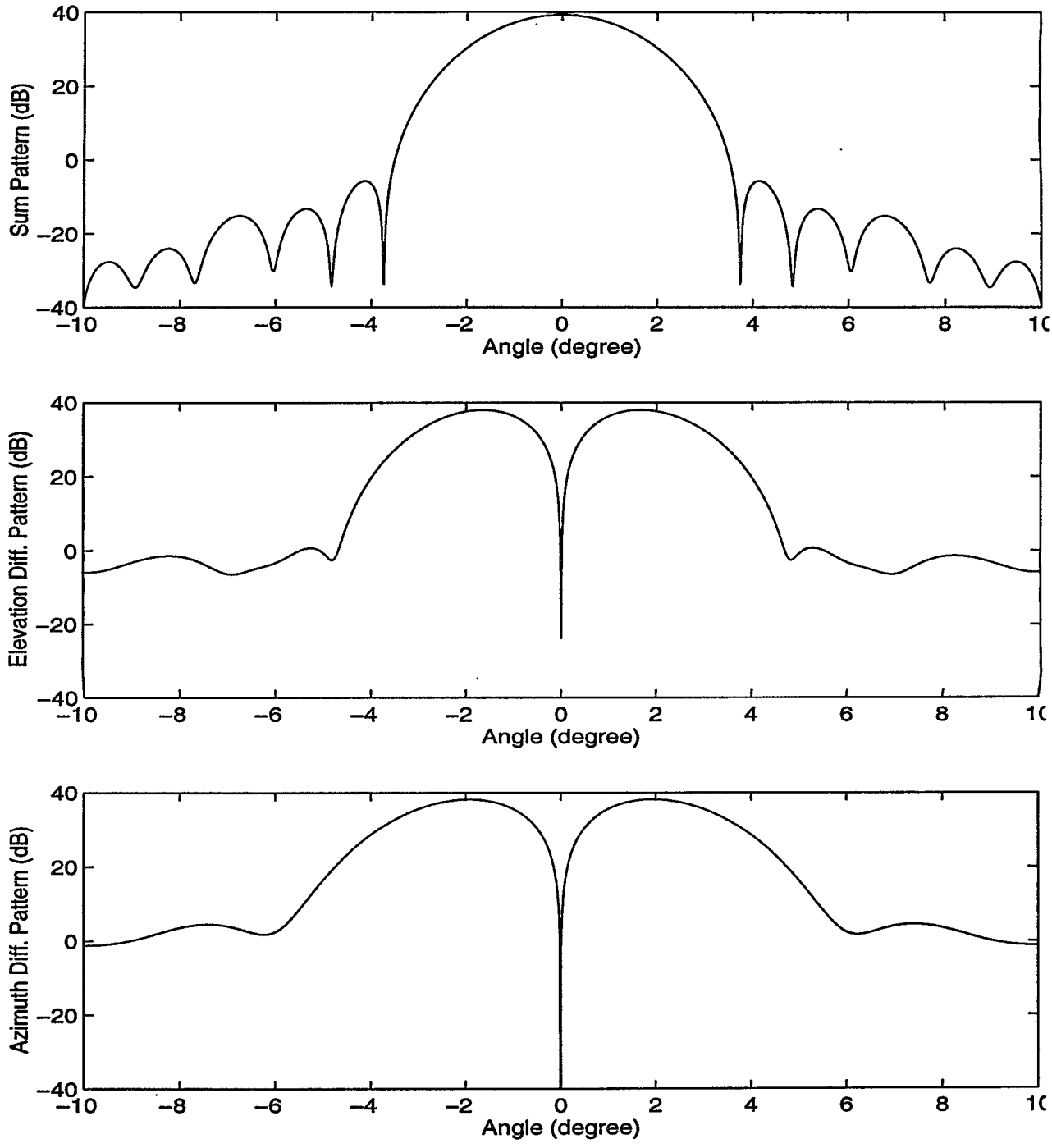

Figure 5 Sum and difference channels for the simulated phased array antenna.

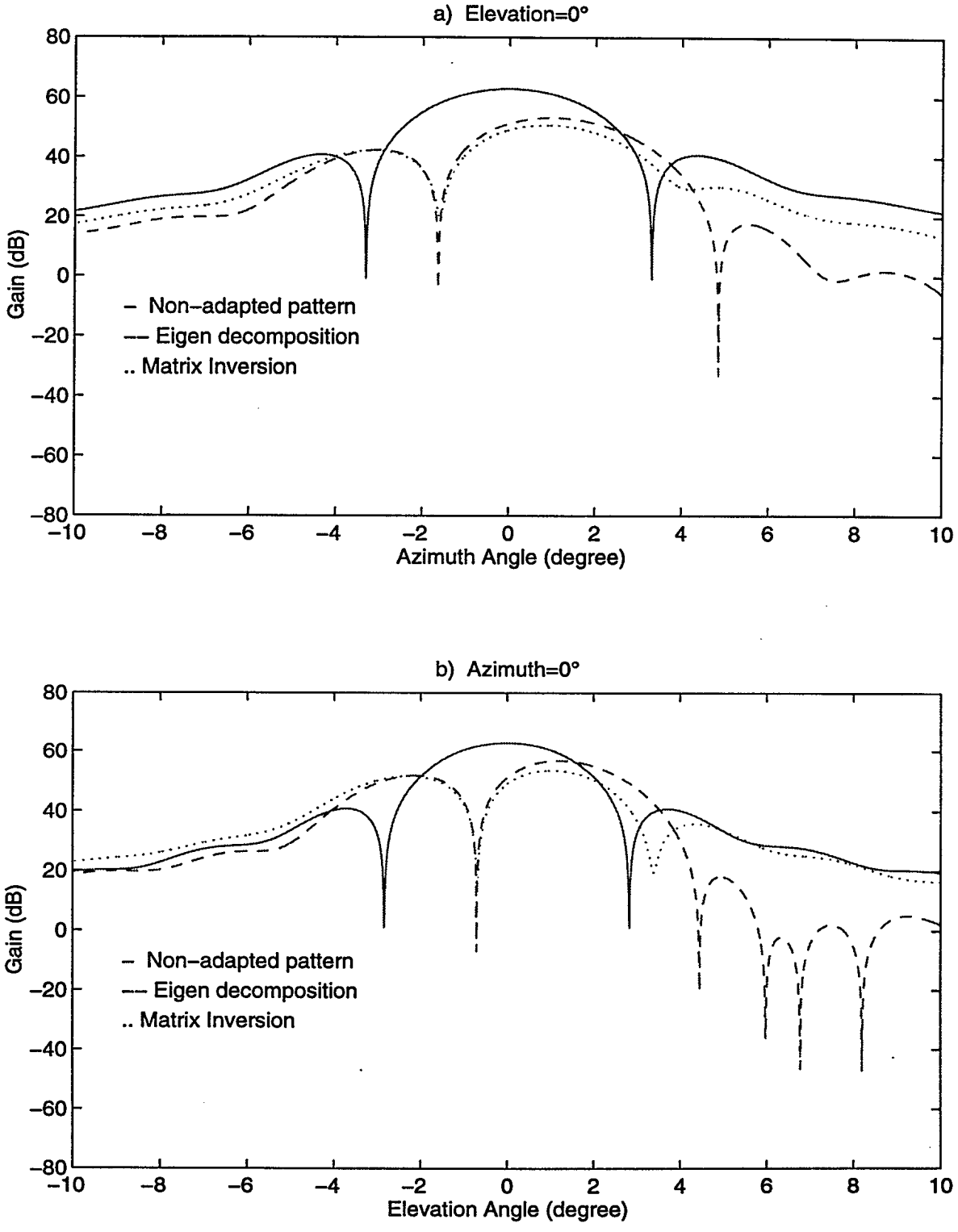

Figure 6 Adapted antenna patterns for mainbeam jamming scenario.

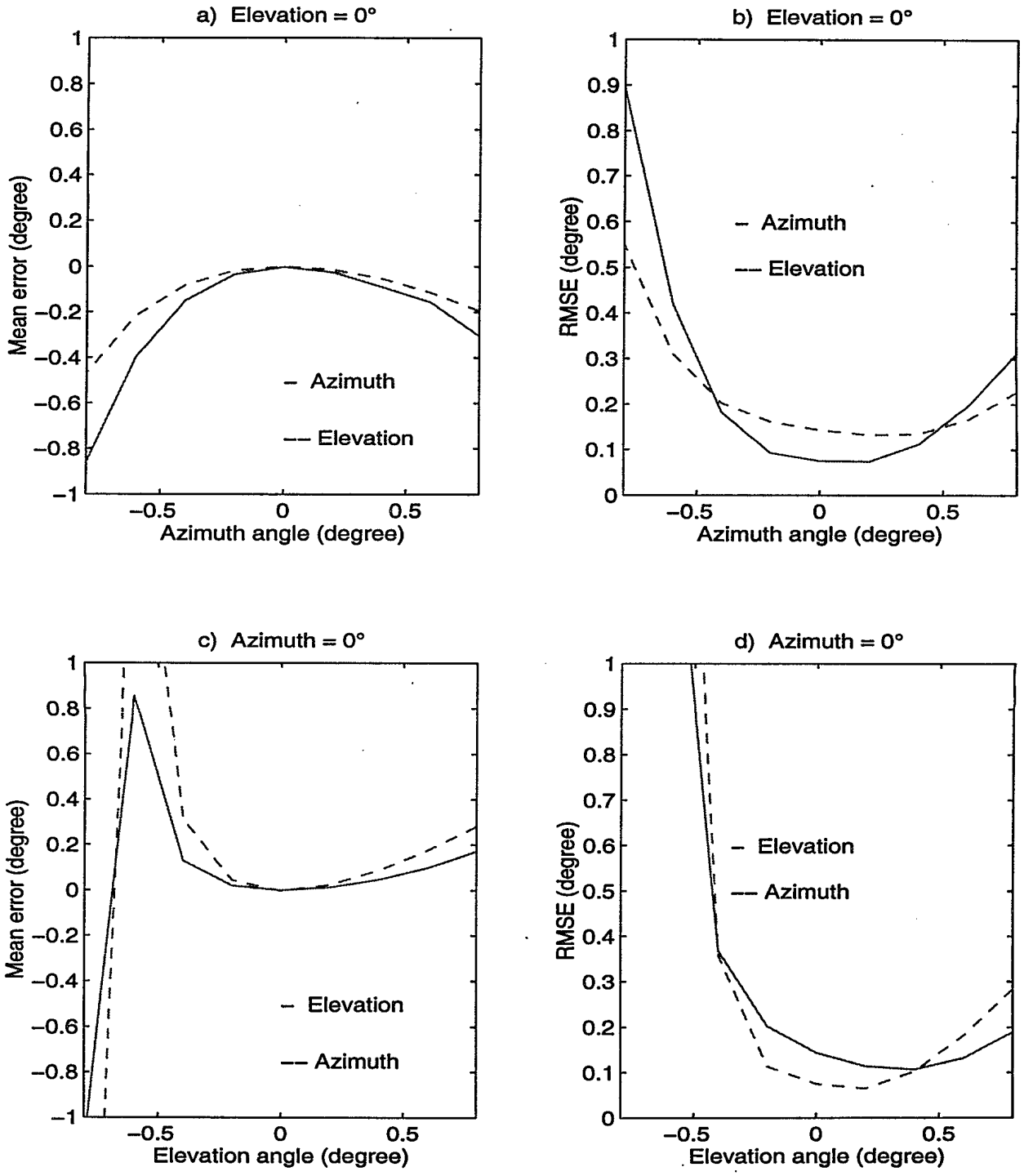

Figure 7 Mean Error and RMSE of CAM with eigendecomposition for mainbeam jamming scenario.

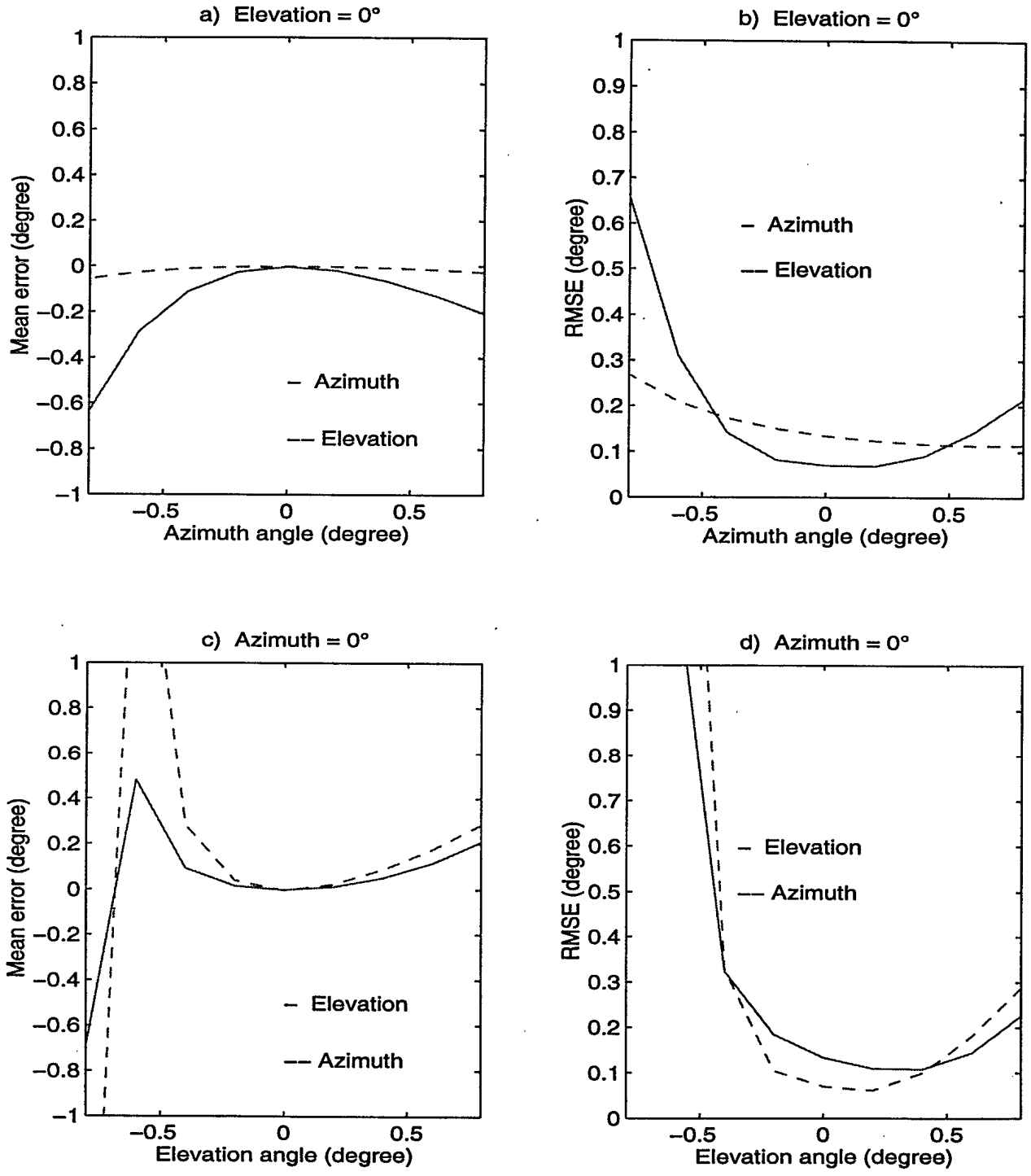

Figure 8 Mean Error and RMSE of CAM technique with SMI for mainbeam jamming scenario.

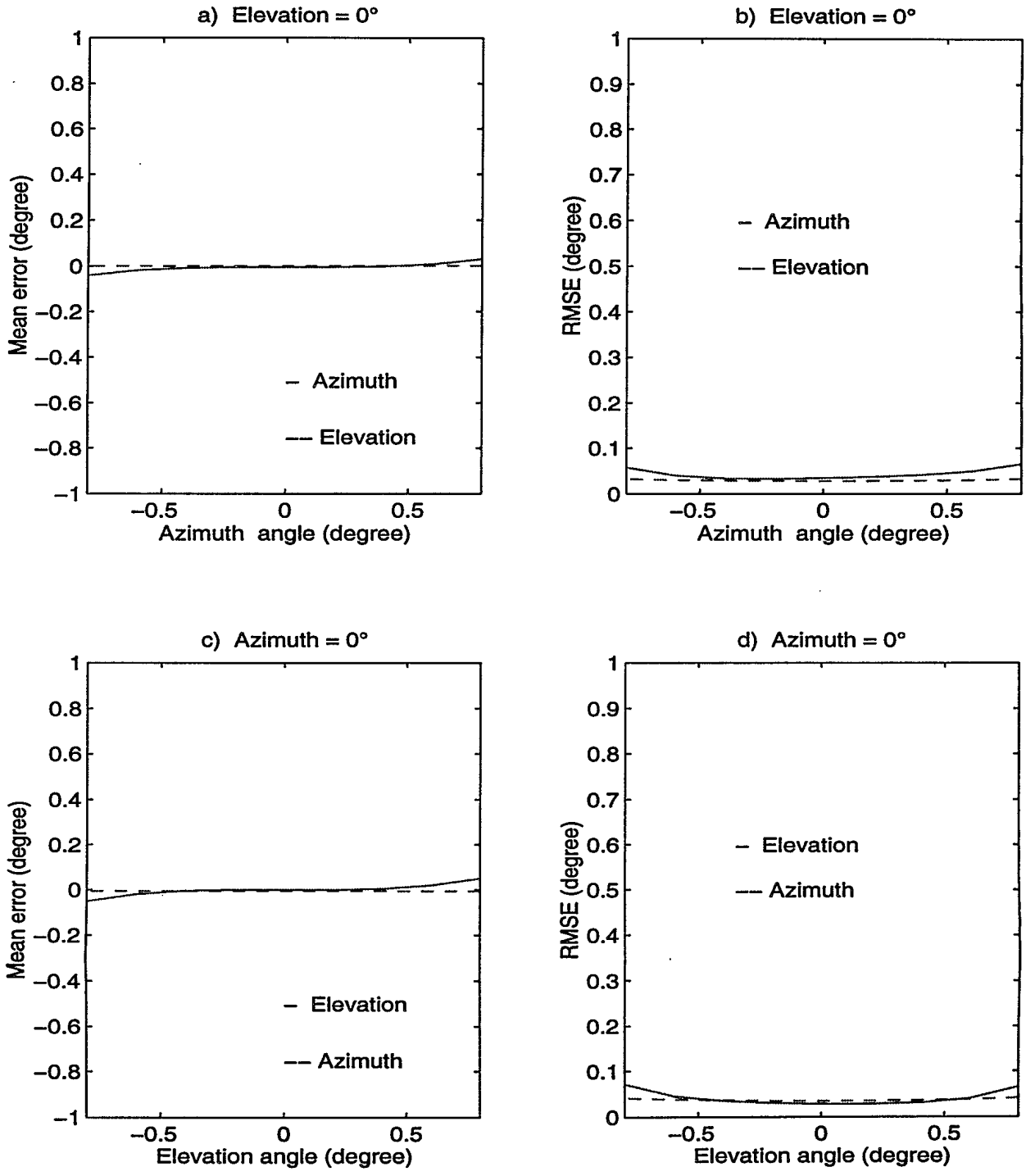

Figure 9 Mean Error and RMSE of conventional monopulse for medium-level sidelobe jamming.

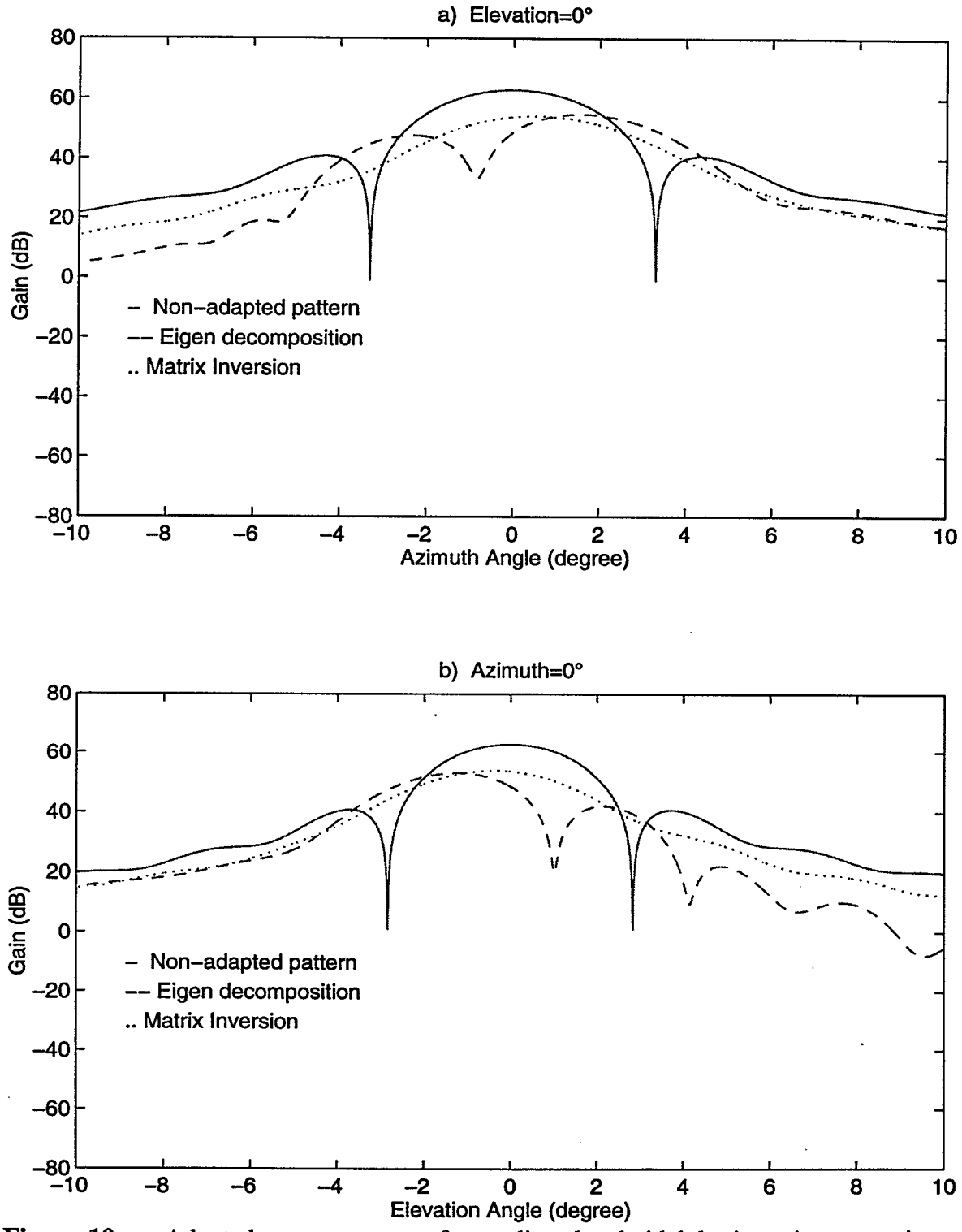

Figure 10 Adapted antenna pattern for medium-level sidelobe jamming scenario.

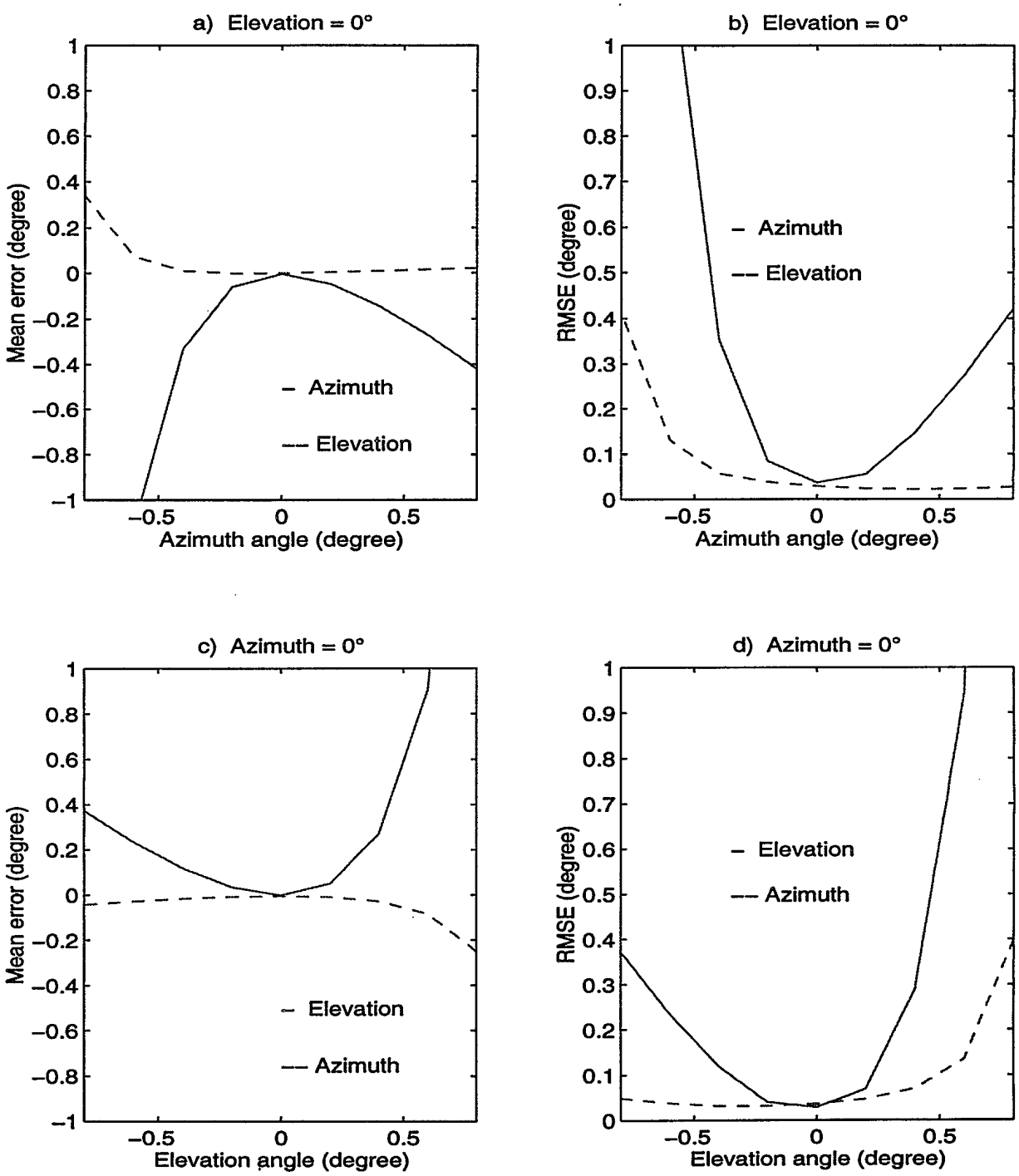

Figure 11 Mean Error and RMSE of CAM with eigendecomposition for medium-level sidelobe jamming scenario.

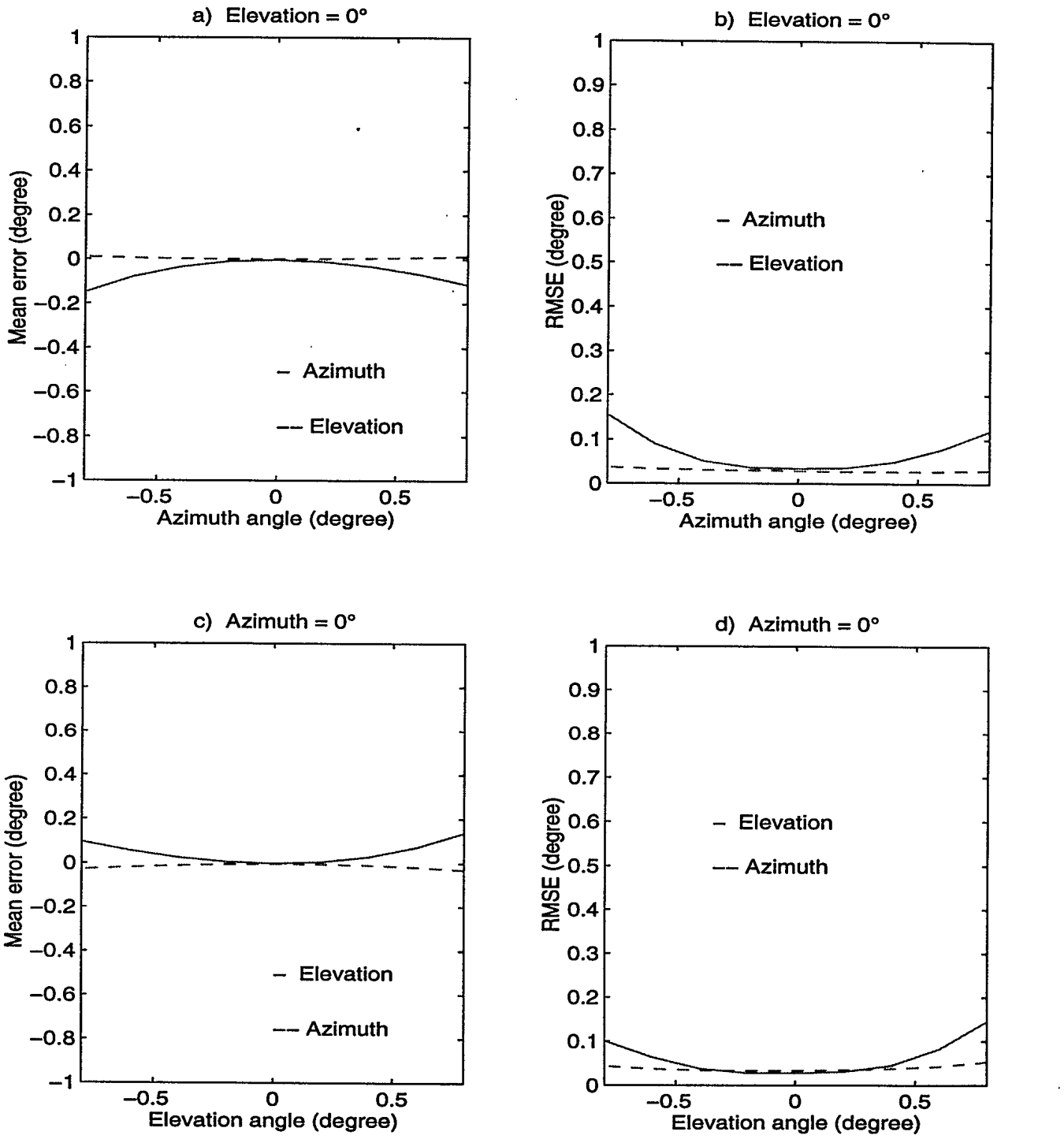

Figure 12 Mean Error and RMSE of CAM technique with SMI for medium-level sidelobe jamming scenario.

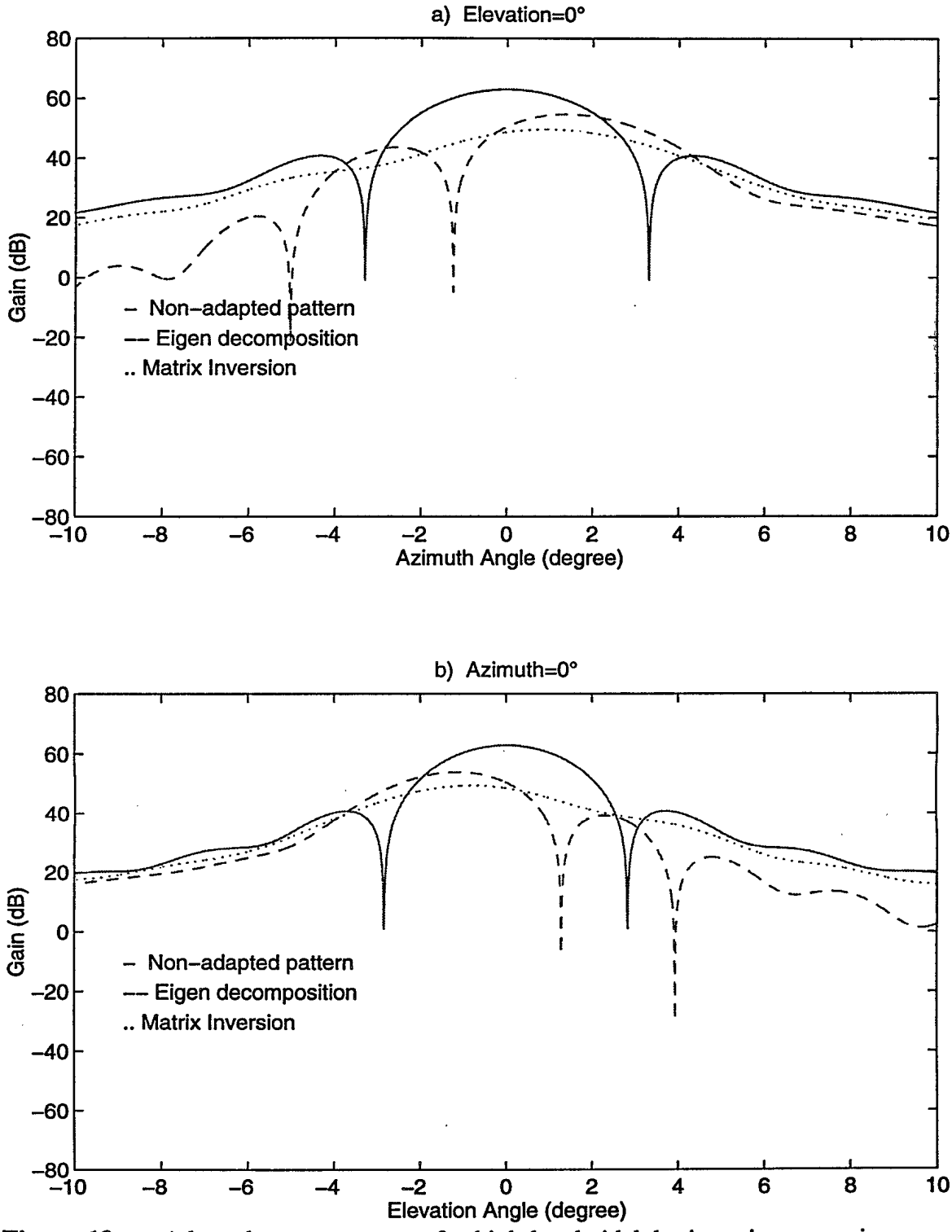

Figure 13 Adapted antenna pattern for high-level sidelobe jamming scenario.

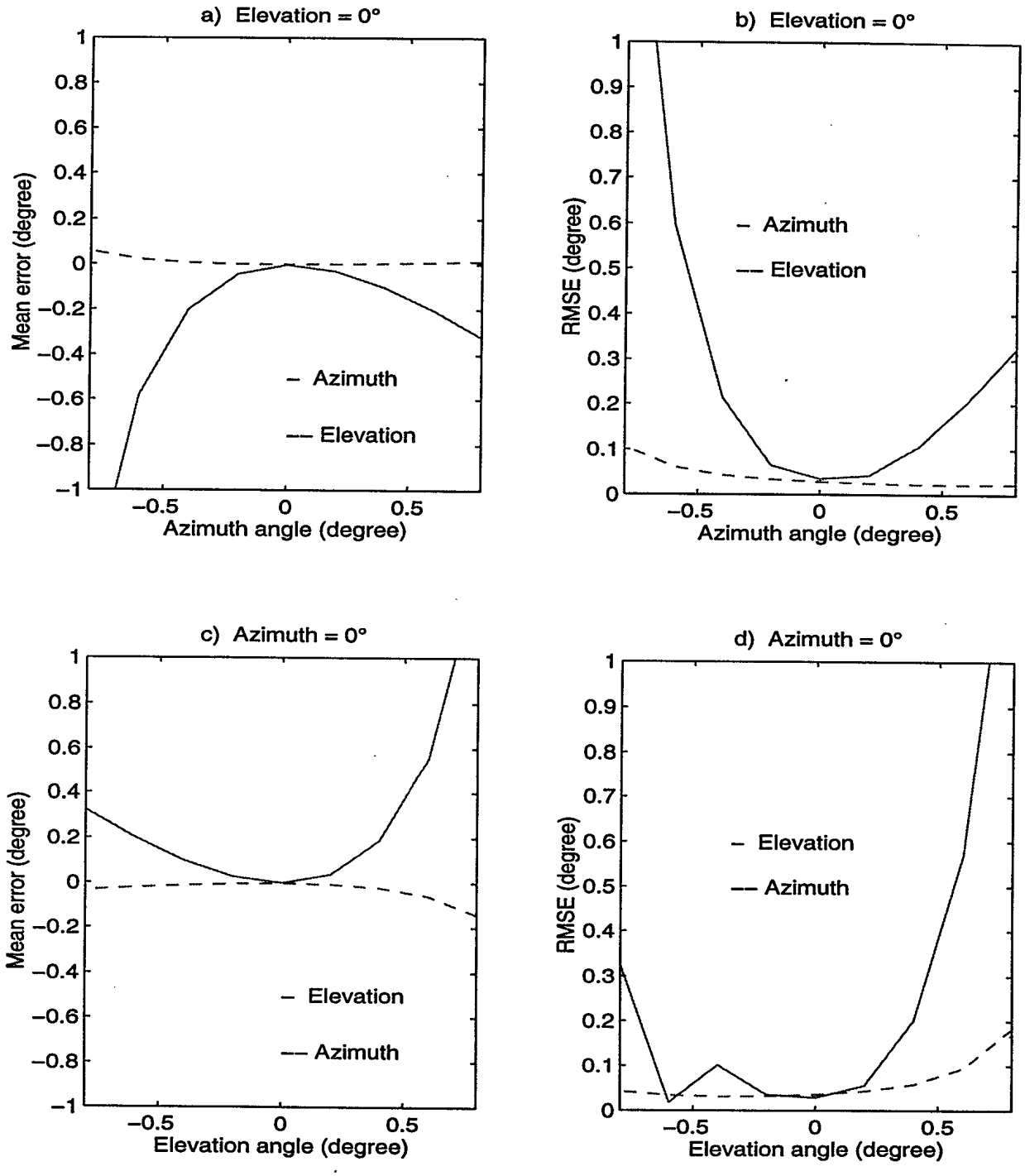

Figure 14 Mean Error and RMSE of CAM technique with eigendecomposition for high-level sidelobe jamming scenario.

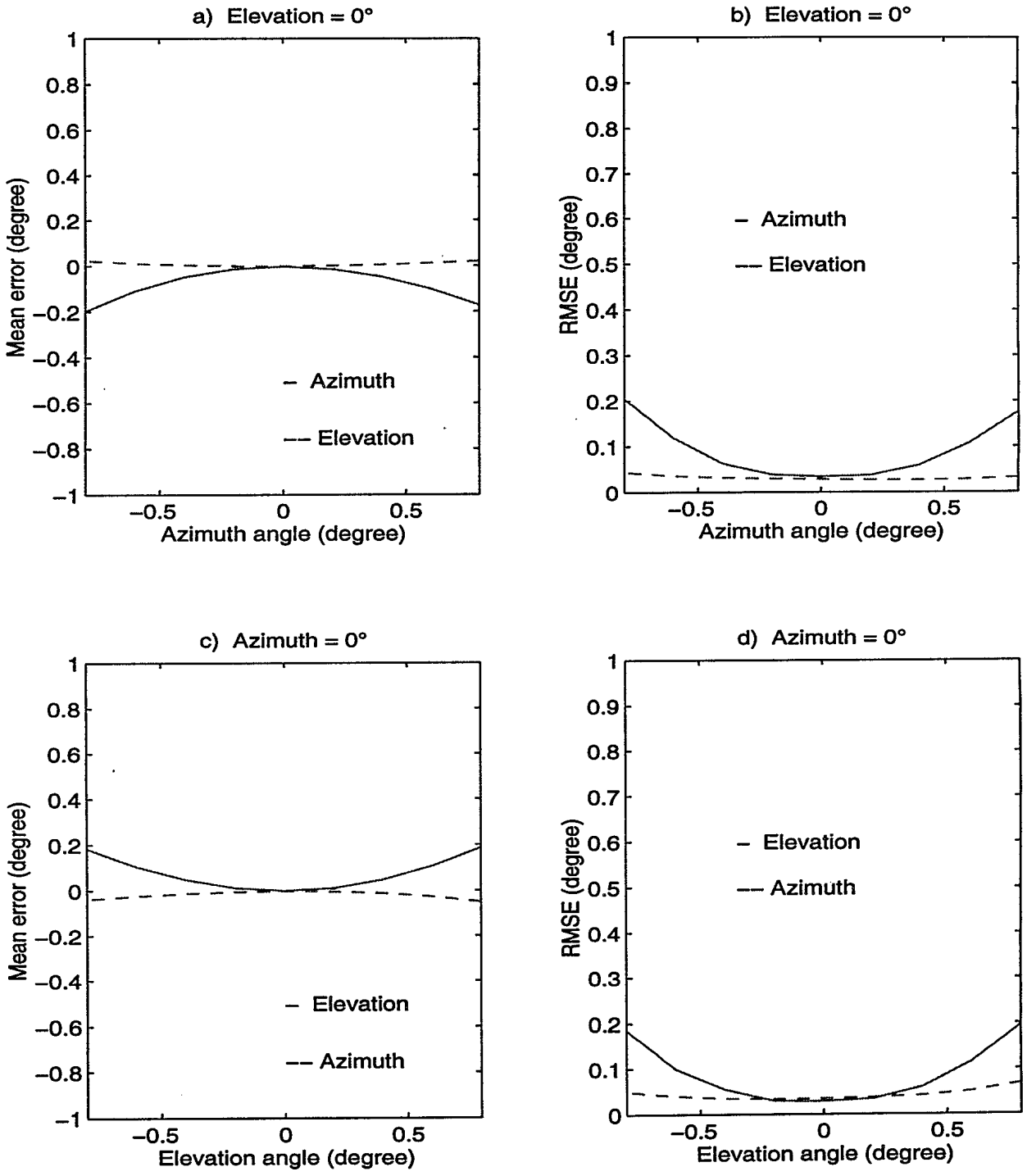

Figure 15 Mean error and RMSE of CAM technique with SMI for high-level sidelobe jamming scenario.

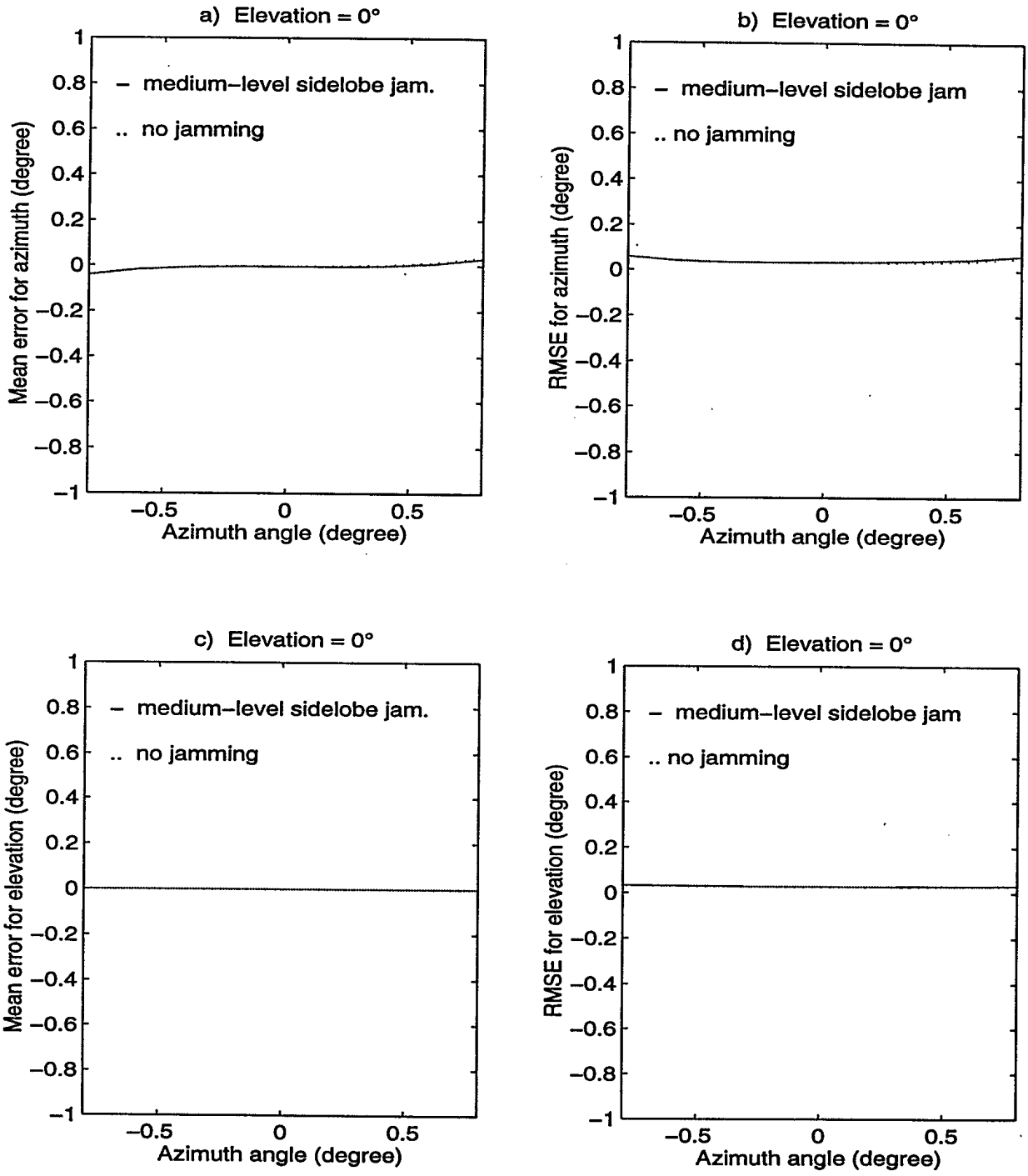

Figure 16 Mean error and RMSE of conventional monopulse for test case 1.

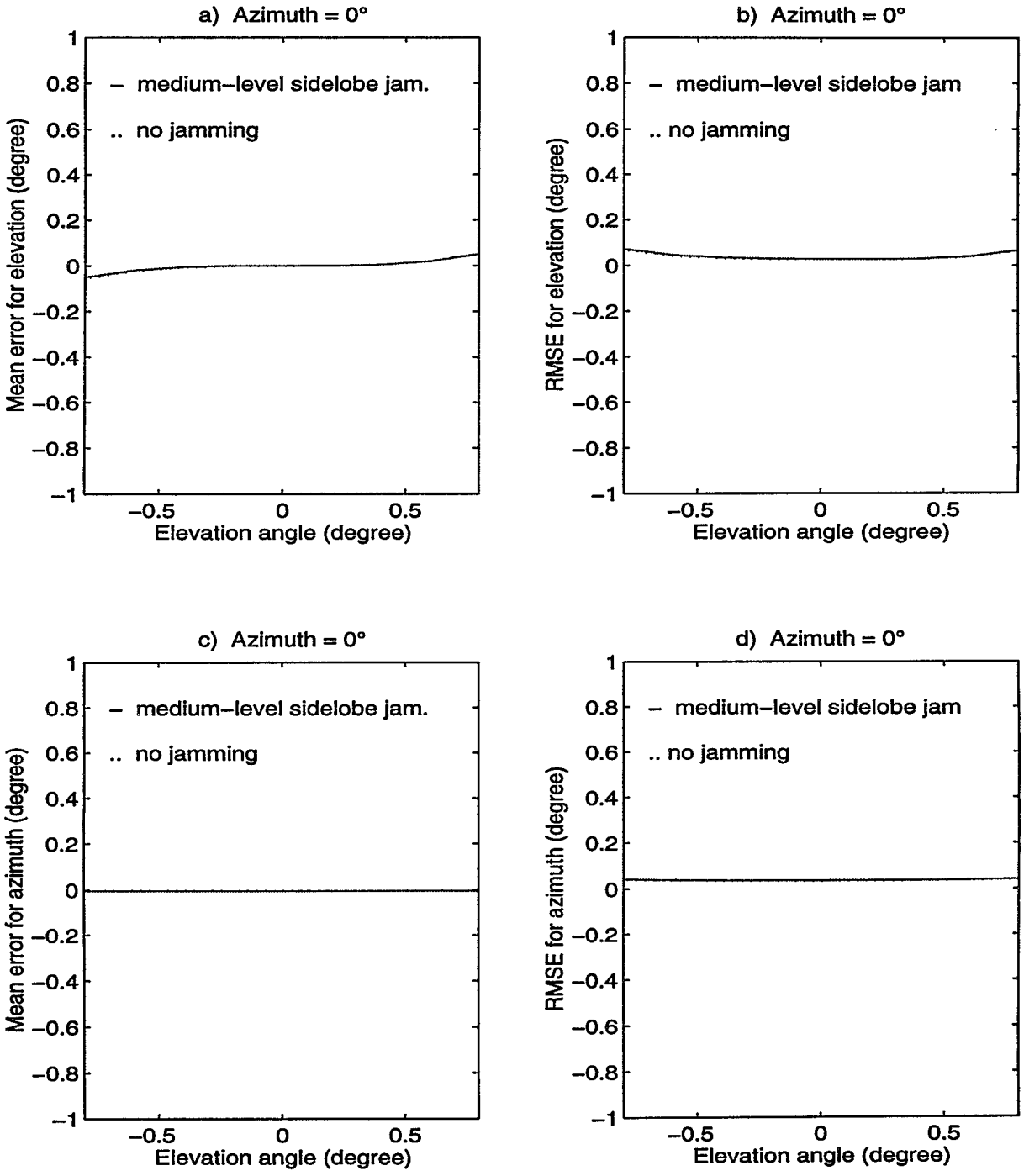

Figure 17 Mean Error and RMSE of conventional monopulse for test case 2.

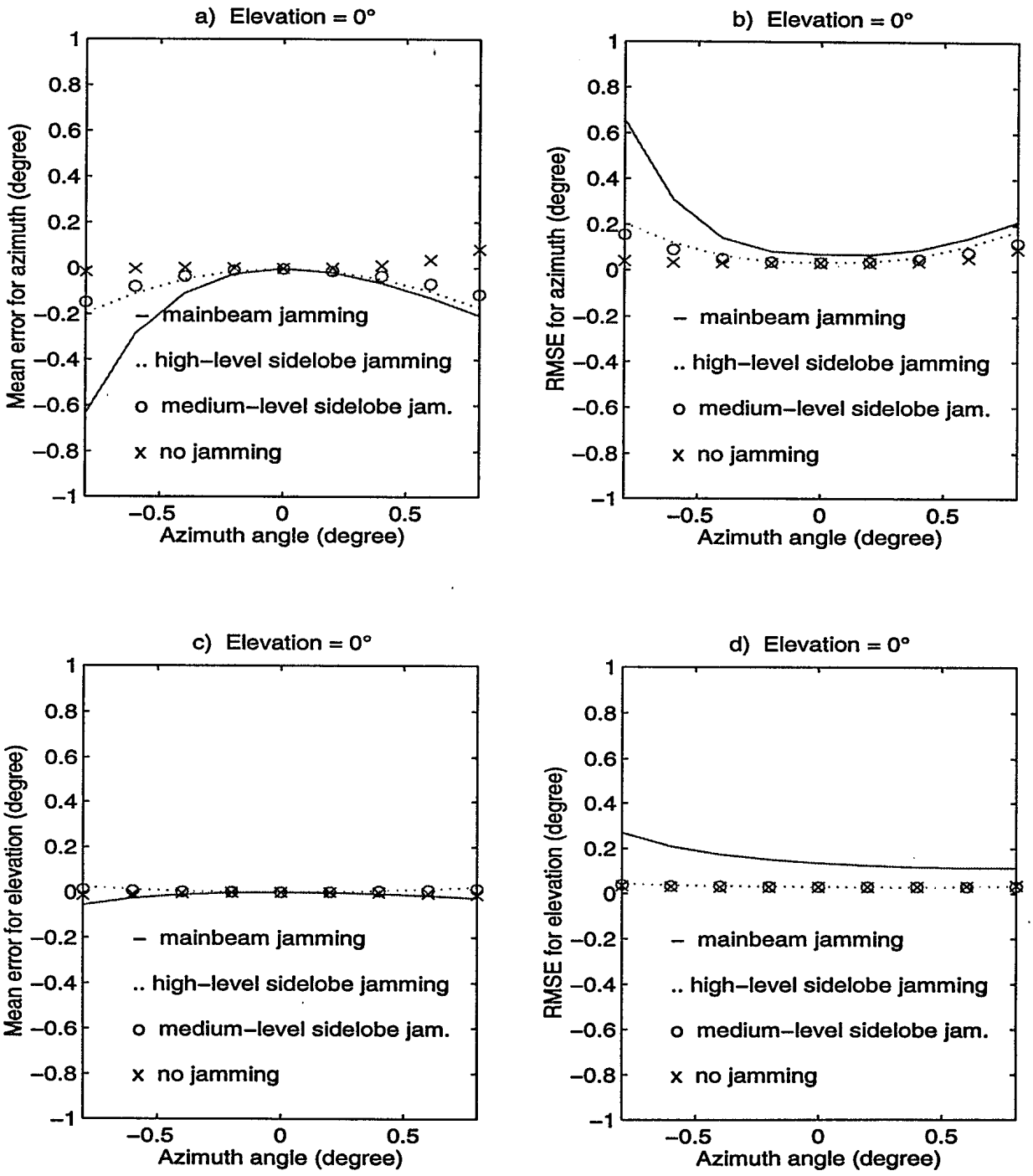

Figure 18 Mean Error and RMSE of CAM with SMI for all scenarios, test case 1.

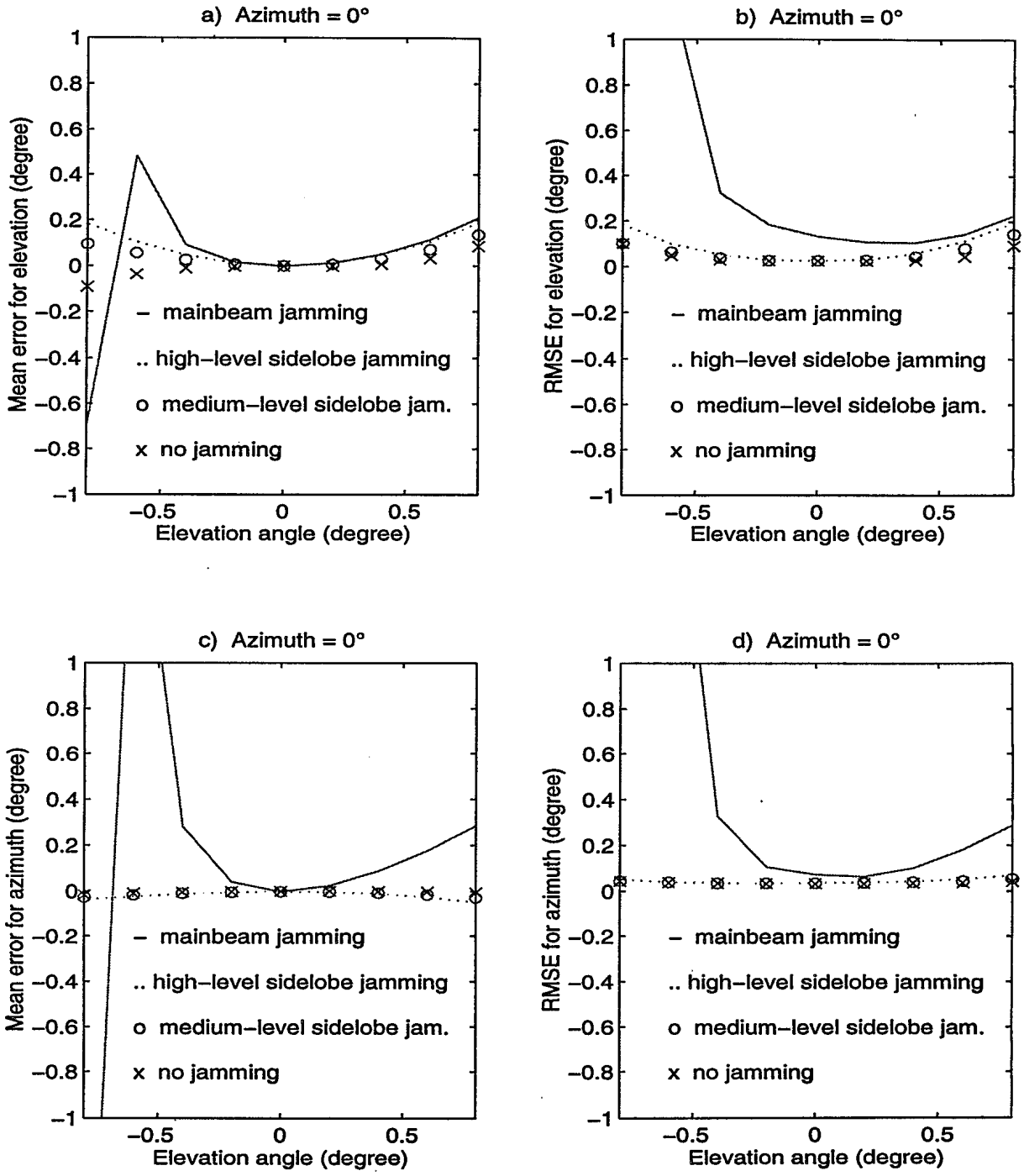

Figure 19 Mean error and RMSE of CAM technique with SMI for all scenarios, test case 2.

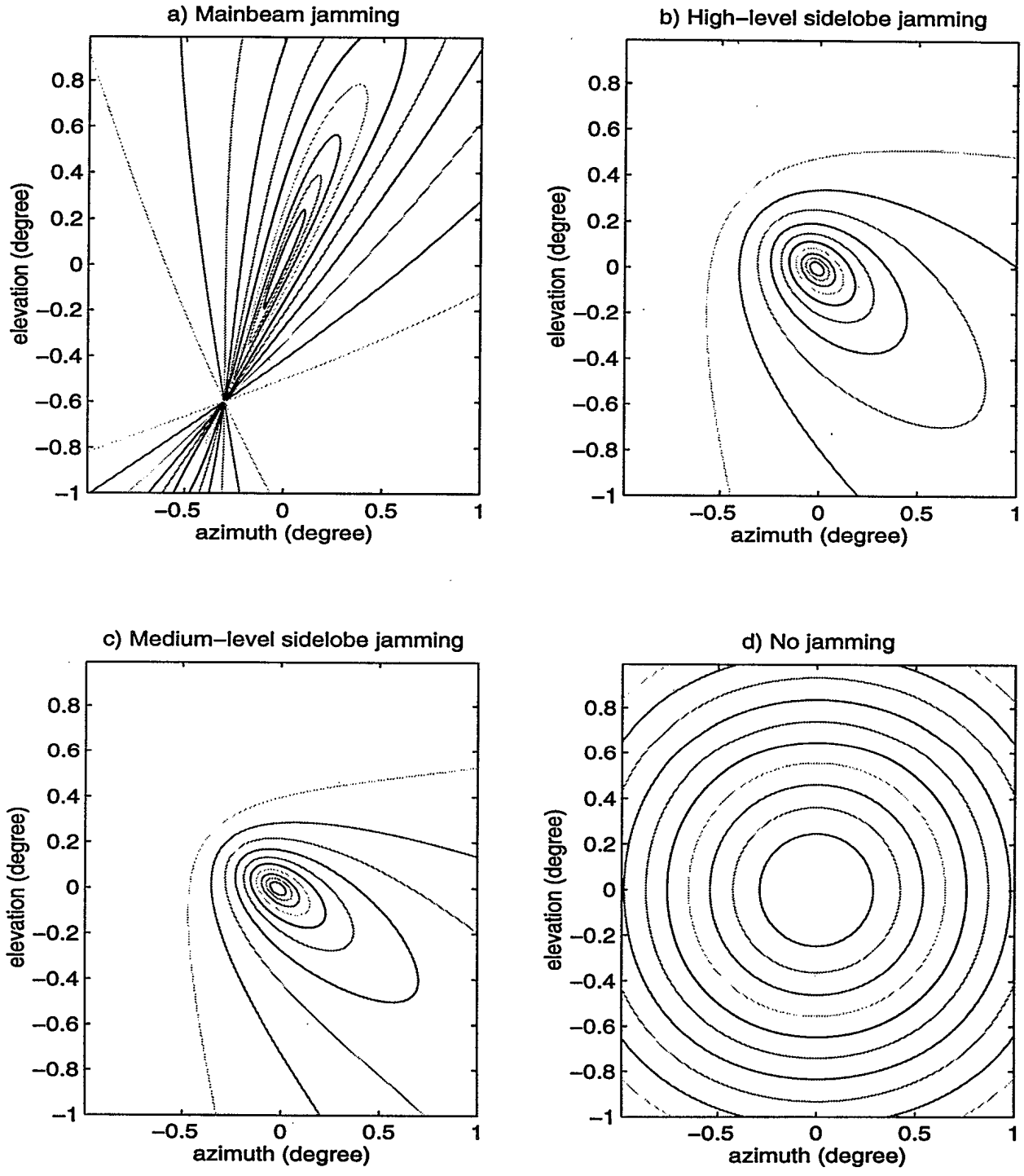

Figure 20 Contour plots of MMUSIC for all scenarios.

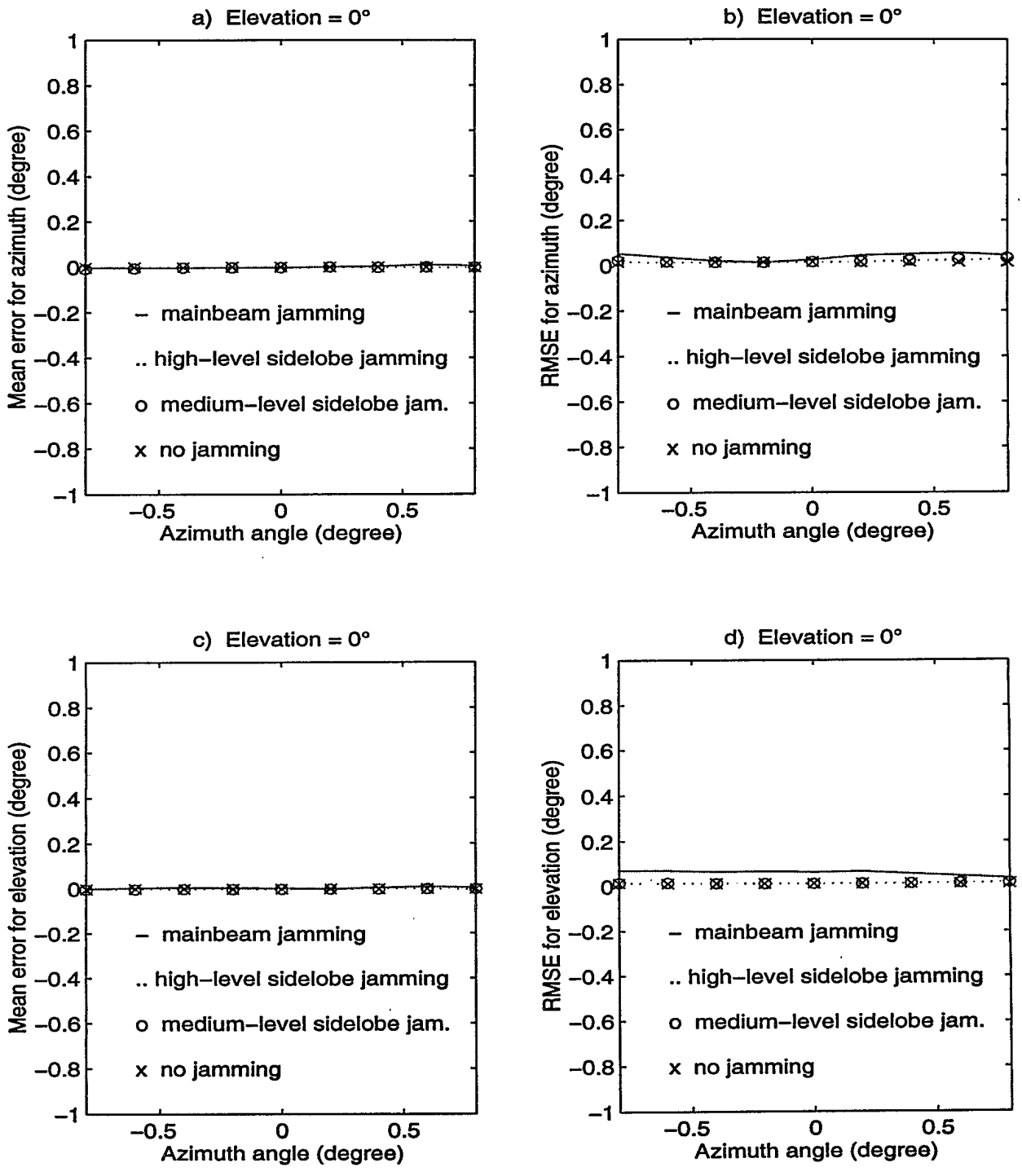

Figure 21 Mean error and RMSE of MMUSIC for all scenarios, test case 1.

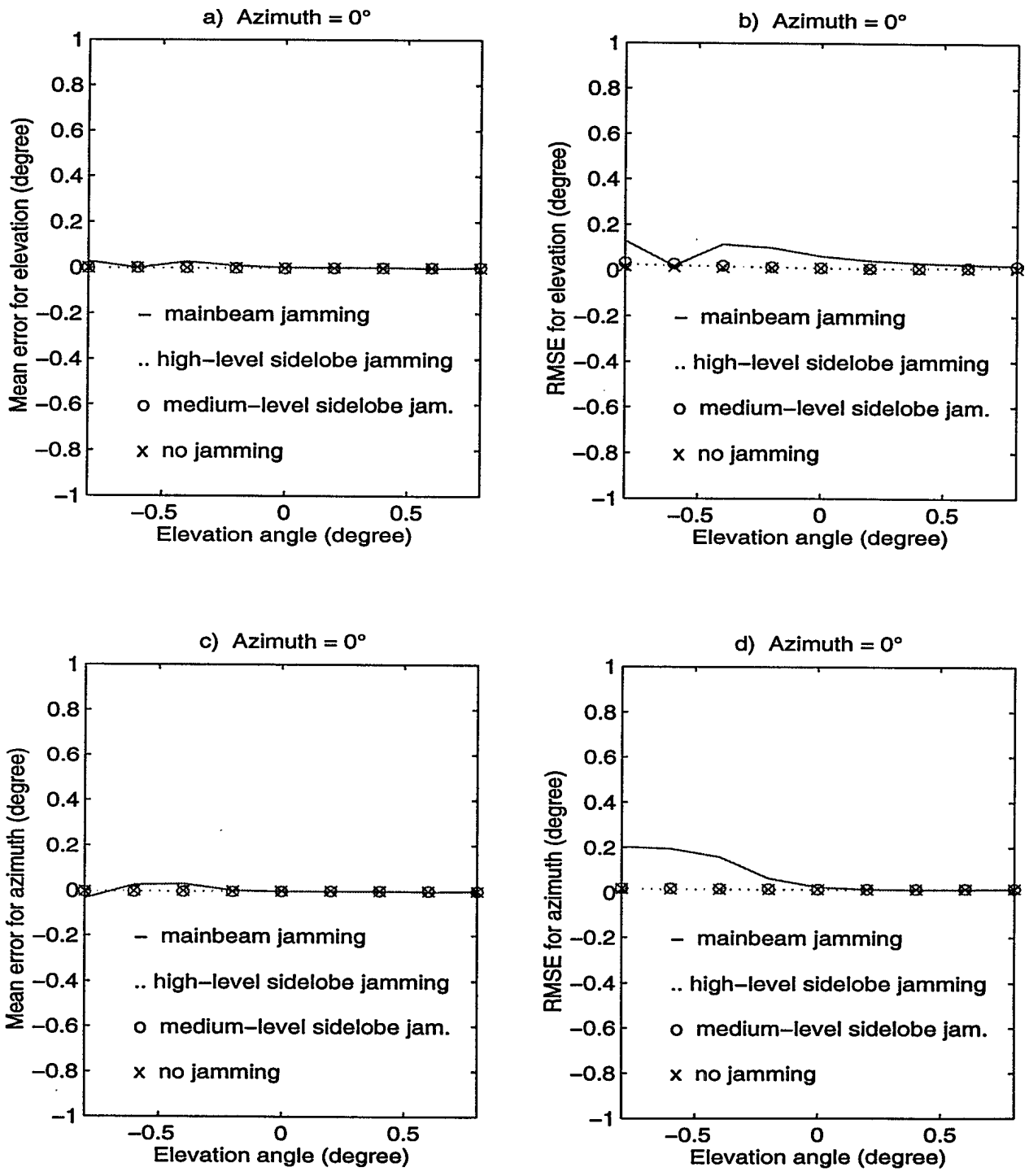

Figure 22 Mean error and RMSE of MMUSIC for all scenarios, test case 2.

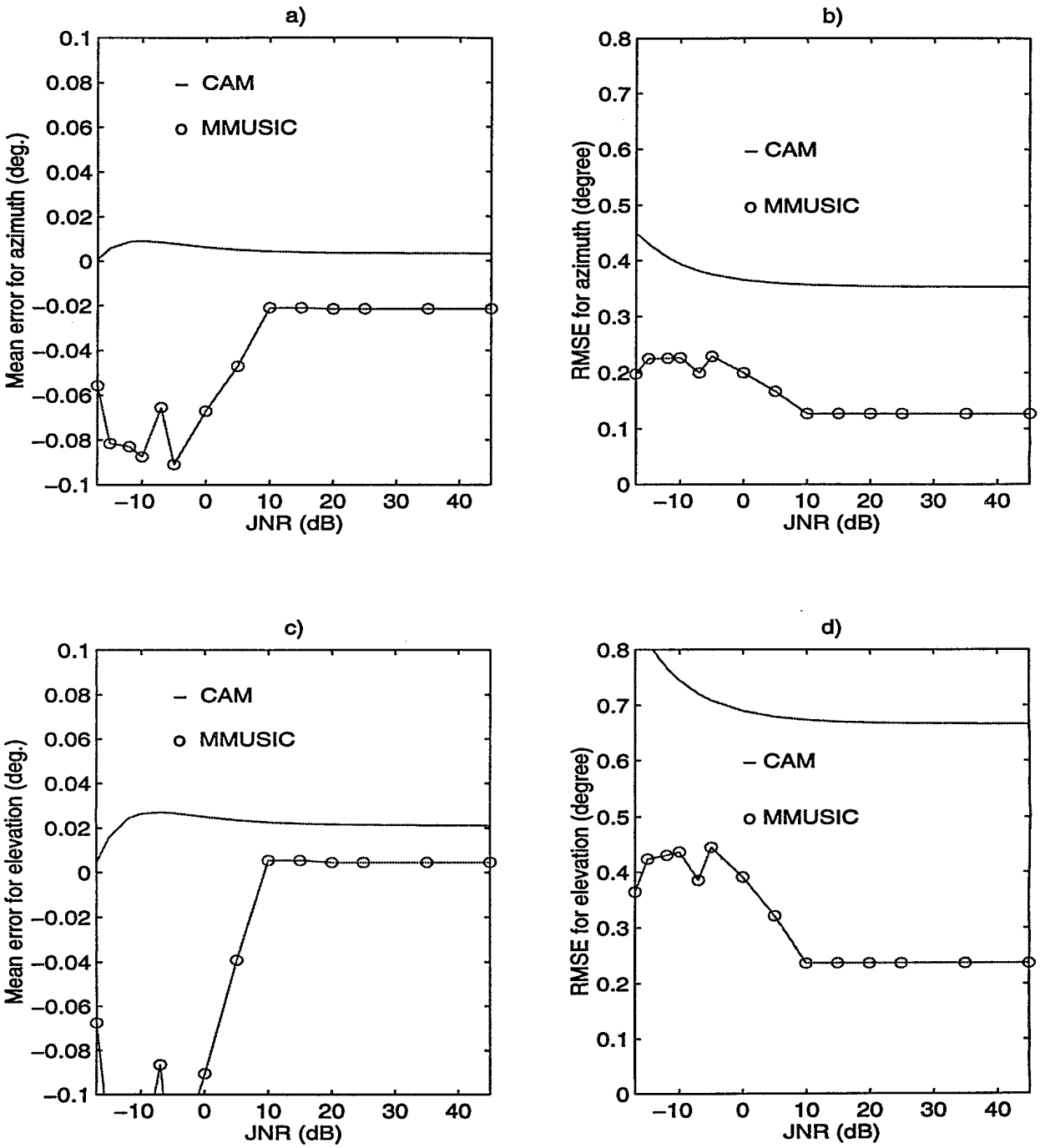

Figure 23 Mean error and RMSE vs Jammer-to-Noise Ratio for SNR=-17 dB.

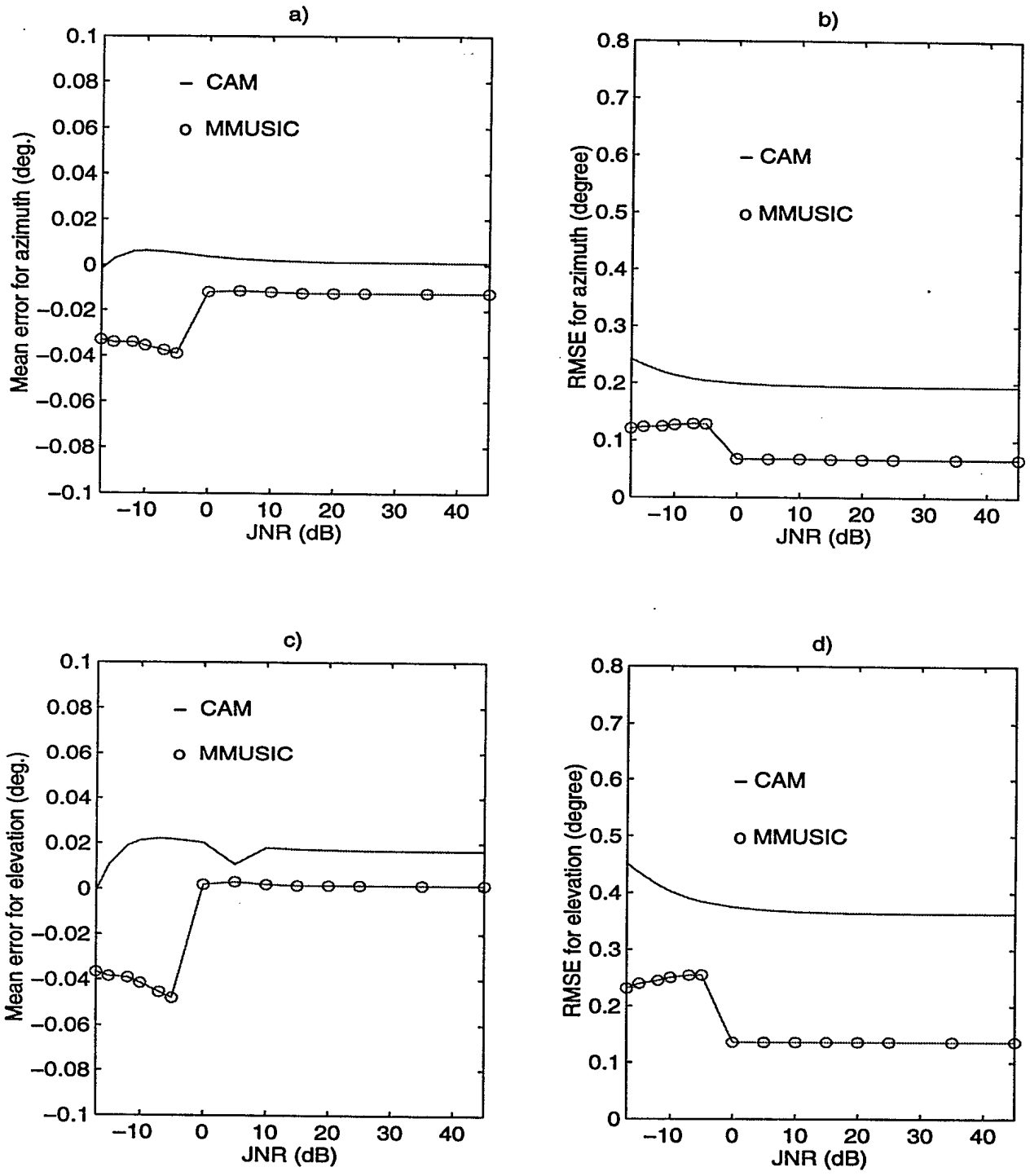

Figure 24 Mean error and RMSE vs Jammer-to-Noise Ratio for SNR=-12 dB.

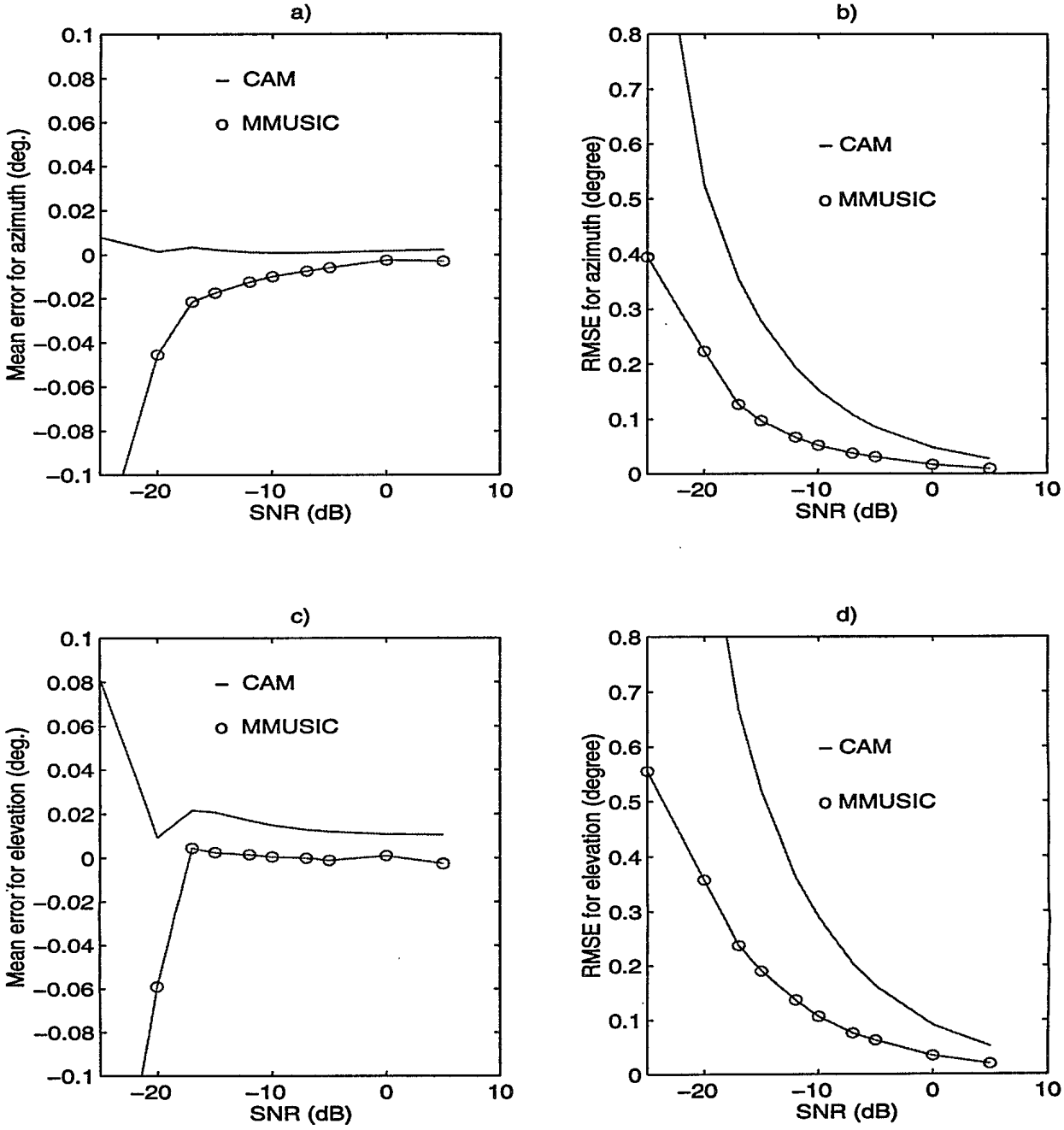

Figure 25 Mean error and RMSE vs Signal-to-Noise Ratio for JNR=25 dB.

UNCLASSIFIED

SECURITY CLASSIFICATION OF FORM
(highest classification of Title, Abstract, Keywords)

DOCUMENT CONTROL DATA

(Security classification of title, body of abstract and indexing annotation must be entered when the overall document is classified)

1. ORIGINATOR (the name and address of the organization preparing the document. Organizations for whom the document was prepared, e.g. Establishment sponsoring a contractor's report, or tasking agency, are entered in section 8.)

Defence Research Establishment Ottawa

2. SECURITY CLASSIFICATION (overall security classification of the document. including special warning terms if applicable)

UNCLASSIFIED

3. TITLE (the complete document title as indicated on the title page. Its classification should be indicated by the appropriate abbreviation (S,C,R or U) in parentheses after the title.)

Estimation of Target Angular Position Under Mainbeam Jamming Conditions (U)

4. AUTHORS (Last name, first name, middle initial)

Toulgat, Mylène and Turner, Ross M.

5. DATE OF PUBLICATION (month and year of publication of document)

Dec 95

6a. NO. OF PAGES (total containing information. Include Annexes, Appendices, etc.)

6b. NO. OF REFS (total cited in document)

7. DESCRIPTIVE NOTES (the category of the document, e.g. technical report, technical note or memorandum. If appropriate, enter the type of report, e.g. interim, progress, summary, annual or final. Give the inclusive dates when a specific reporting period is covered.)

Technical Report

8. SPONSORING ACTIVITY (the name of the department project office or laboratory sponsoring the research and development. Include the address.)

DREO

9a. PROJECT OR GRANT NO. (if appropriate, the applicable research and development project or grant number under which the document was written. Please specify whether project or grant)

01A01

9b. CONTRACT NO. (if appropriate, the applicable number under which the document was written)

10a. ORIGINATOR'S DOCUMENT NUMBER (the official document number by which the document is identified by the originating activity. This number must be unique to this document.)

DREO REPORT 1281

10b. OTHER DOCUMENT NOS. (Any other numbers which may be assigned this document either by the originator or by the sponsor)

11. DOCUMENT AVAILABILITY (any limitations on further dissemination of the document, other than those imposed by security classification)

(X) Unlimited distribution
( ) Distribution limited to defence departments and defence contractors; further distribution only as approved
( ) Distribution limited to defence departments and Canadian defence contractors; further distribution only as approved
( ) Distribution limited to government departments and agencies; further distribution only as approved
( ) Distribution limited to defence departments; further distribution only as approved
( ) Other (please specify):

12. DOCUMENT ANNOUNCEMENT (any limitation to the bibliographic announcement of this document. This will normally correspond to the Document Availabilty (11). However, where further distribution (beyond the audience specified in 11) is possible, a wider announcement audience may be selected.)

UNCLASSIFIED

SECURITY CLASSIFICATION OF FORM

13. ABSTRACT (a brief and factual summary of the document. It may also appear elsewhere in the body of the document itself. It is highly desirable that the abstract of classified documents be unclassified. Each paragraph of the abstract shall begin with an indication of the security classification of the information in the paragraph (unless the document itself is unclassified) represented as (S), (C), (R), or (U). It is not necessary to include here abstracts in both offical languages unless the text is bilingual).

A phased-array multifunction radar (MFR) with an agile pencil beam will invariably employ a monopulse system for precise angle measurement. Such a monopulse system has three receiver channels, one channel for each of the sum, azimuth and elevation difference beamformers. This report considers a modest expansion of the number of receiving channels from three to five channels. The five channels form an adaptive array which can be used to provide mainbeam nulling of jammers. A new algorithmic approach to mainbeam jammer nulling and target angle estimation is applied to this five-element adaptive array. With this algorithm, the jammer subspace is first evaluated by sampling at ranges where the target is absent (e.g. beyond the maximum range of targets or during a quiet period when the radar is not transmitting). Data vectors are then processed to remove the jammer thus allowing the target to be detected. Finally a high resolution technique, Multiple Signal Classification (MUSIC), is used to estime the target Drection-Of-Arrival)DOA) from the processed data vectors. The model used in the MUSIC technique takes into account the fact that the jammer has been cancelled in the target data vector. The performance of this algorithm is evaluated through simulations and compared with the Corrected Adaptive Monopulse (CAM) (3,4) for a typical X-band phased array. The new algorithm provides more accurate estimates than CAM when the target is close to the jammer, at the expense of a large computational load.

14. KEYWORDS, DESCRIPTORS or IDENTIFIERS (technically meaningful terms or short phrases that characterize a document and could be helpful in cataloguing the document. They should be selected so that no security classification is required. Identifiers, such as equipment model designation, trade name, military project code name, geographic location may also be included. If possible keywords should be selected from a published thesaurus. e.g. Thesaurus of Engineering and Scientific Terms (TEST) and that thesaurus-identified. If it is not possible to select indexing terms which are Unclassified, the classification of each should be indicated as with the title.)

Phased array
Mainbeam jamming
Estimation of Direction-of-Arrival
Multifunction Radar
Radar

UNCLASSIFIED

SECURITY CLASSIFICATION OF FORM

155549